

Major Late Pleistocene explosive eruptions of Changbaishan and Japanese volcanoes revealed by a 100-ka tephra record from the Sea of Japan

Jia Chen^{a,b}, Chunqing Sun^{b,*}, Yang Li^{a,*}, Yuxin Chen^{b,c}, Shuang Zhang^d, Zhengfu Guo^b, Jiaqi Liu^b

^a School of Geography and Resource Science, Sichuan Normal University, Chengdu, China

^b Key Laboratory of Cenozoic Geology and Environment, Institute of Geology and Geophysics, Chinese Academy of Sciences, Beijing, China

^c School of Earth and Space Science, University of Science and Technology of China, Hefei, China

^d Department of Geography, Royal Holloway University of London, Egham, UK



ARTICLE INFO

Editor name: Prof. M Elliot

Keywords:

Changbaishan

B-J

B-Ym

Tianwenfeng

Aso-4

Aira

ABSTRACT

The many subaerial volcanoes around northeast Asia have experienced frequent large-magnitude eruptions. However, many of them are not fully characterized geochronologically and geochemically, such as Changbaishan on the border between China and North Korea. We identified ten tephra layers in marine sediment cores from the Sea of Japan, confirming the occurrence of seven major eruptions around northeast Asia over the past 100 ka. Three of the tephra layers are major marker horizons around northeast Asia: AT (~30 ka), Aso-4 (~86 ka), and Toya (~108 ka), which were used to constrain age models of the sediment cores. A pre-AT tephra, possibly correlative with the A-Kn eruption of the Aira caldera, was recognized in the central Sea of Japan, and it is linked to the high-resolution sedimentary record of Lake Suigetsu. The fourth Aso-4 component was recognized in this study, while component 3 was not recognized in the sediment cores from the Sea of Japan, suggesting that the eruption and tephra dispersal processes of the ~86 ka Aso-4 eruption were complex. Additionally, one tephra layer with the age of 92.0–86.1 ka was identified in the eastern Sea of Japan; it had a similar composition to the BT-30 tephra recorded in Lake Biwa, indicating that it can serve as a new marker horizon from the Sea of Japan to central Japan. For the first time, the Changbaishan Tianwenfeng eruption was correlated with the B-J tephra from the Sea of Japan, based on a robust geochemical correlation between distal and proximal records, and was dated to 60.1–47.3/53.8–42.7 ka based on the age models of the marine sediment cores. The B-Ym tephra with an age of 87.3–81.8 ka recorded in the eastern Sea of Japan was correlated to the Changbaishan tephra, but the source eruption was not determined. These two tephra layers could be used as potential regional marker horizons when considering their thickness present in the marine sediments of the Sea of Japan.

1. Introduction

Refining the volcanic eruption history is fundamental for understanding eruptive frequency and volcanic hazards assessment (Lindsay and Robertson, 2018; Rawson et al., 2015). Reconstructing the eruptive history of an individual volcano is determined by establishing the sequences and eruption timings of the ejecta. Over the past few decades, various dating methods have been developed to date Quaternary volcanic deposits; however, determining the precise eruption timing of a volcanic deposit is often based on a combination of different methods, as each method has its own limitations (Fattah and Stokes, 2003). For example, radiocarbon (^{14}C) analysis is only applicable to dating eruptive

deposits younger than ~40–50 ka and containing organic material.

Japan is one of the most volcanic active regions of the world (Newhall et al., 2018). Explosive eruptions from Japan generate widespread tephra marker horizons around northeast Asia and even northern hemisphere, such as their ashes have been detected in Greenland ice sheet, northern America and low latitude Asia (Albert et al., 2019, 2024; Bourne et al., 2016; Davies et al., 2024; Machida and Arai, 2003; Mackay et al., 2016; Sun et al., 2021, 2022). During the Late Pleistocene, ~30 ka AT and ~86 ka Aso-4 are the most widespread marker horizons for comparing Sea of Japan marine sediments (Ikehara, 2015). Recent distal cryptotephra identifications confirmed that there are several explosive eruptions before the ~30 ka AT eruption, which was detected in the Sea

* Corresponding authors.

E-mail addresses: suncq@mail.igcas.ac.cn (C. Sun), li.yang@sicnu.edu.cn (Y. Li).

of Japan sediments (Machida and Arai, 2003; McLean et al., 2020a, 2020b). Aso-4 is characterized by its highly heterogeneous glass compositions ranging from less evolved trachytic to dacitic glass shards to evolved rhyolitic shards, however, the less evolved trachytic to dacitic member was not found in the distal records from Lake Suigetsu northeast to the volcanic vent (Albert et al., 2019; Aoki, 2008; Keller et al., 2021, 2023a, 2023b). Such geochemical discrepancies between distal and proximal records illustrate complex tephra dispersal from this eruption, and thus more distal records are needed to depict such processes. Additionally, more and more distal records revealed several unknown explosive eruptions from Japanese volcanoes which might not be perceived or detected in proximal exposures (Albert et al., 2024; McLean et al., 2020a, 2020b; Vineberg et al., 2024; Sun et al., 2024), suggesting that full explosive eruptive history of this region is still not complete.

Aside from the highly active Japanese arc volcanoes, Changbaishan, an intraplate stratovolcano located on the border between China and North Korea, is another most hazardous active volcano in northeast Asia. The Millennium eruption (ME, named because it erupted ~ 1000 CE) of Changbaishan was one of the largest eruptions on Earth over the past ~ 2000 years, and its tephra is widely distributed across northeast Asia and it can even be traced to the Greenland icesheet, forming a hemispheric time-equivalent marker horizon for Quaternary studies (Chen and Blockley, 2016; Hughes et al., 2013; McLean et al., 2016, 2018; Sun et al., 2014, 2015). The geochemical characteristics of volcanic gases and hot springs, and seismological evidence for magmatic activity beneath the volcano, are both indicators of potential volcanic activity (Wei et al., 2013; Zhang and Guo, 2018). Therefore, determining the timings of past eruptions based on dating volcanic deposits, and the characterization of the associated tephra dispersals, are crucial for understanding the potential volcanic hazards of a given volcano.

Changbaishan experienced several major explosive eruptions during the Quaternary, evidenced by proximal exposures and records of distal tephra (e.g., Chen and Blockley, 2016; Lim et al., 2013; Liu et al., 2023; McLean et al., 2018; McLean et al., 2020a, 2020b; Sun et al., 2017; Wei et al., 2013; Zhang and Guo, 2015, 2018). Various dating methods have been applied to date the timings of the past eruptions of Changbaishan; for example, the age of the Qixiangzhan eruption was dated to tens of thousands of years ago by ^{40}Ar — ^{39}Ar and K—Ar dating (Channell et al., 2020; Singer et al., 2014; Wei et al., 2013; Yang et al., 2014), and most recently it was precisely constrained to ~8.1 ka by tephrochronological correlations (Sun et al., 2018). Another notable pre-Millennium eruption (also called the Tianwenfeng eruption as it is located at Tianwenfeng peak) produced a ~ 30-m thickness of pyroclastic deposits (including two sub-units known as NS-1 and NS-2) on the summit of the north slope of Changbaishan (Sun et al., 2017). Although several attempts have been made using ^{40}Ar — ^{39}Ar to constrain the age of this eruption (e.g., Yang et al., 2014), it is still unresolved because of the large uncertainties of the dating results and our limited knowledge of the associated tephra dispersal. Tephra records with precise geochemical characterization from sedimentary archives with a robust sedimentary chronological framework can help to overcome these issues.

In this study, we identified ten visible tephra layers in two marine sediment cores from the Sea of Japan and our objectives are to: (1) characterize glass geochemical compositions of the visible tephra layers recorded in the Sea of Japan; (2) refine the major explosive eruptions of Changbaishan volcano and Japanese volcanoes; (3) develop regional tephra marker horizons for correlating and linking marine and terrestrial sediments.

2. Materials and methods

2.1. Study sites and samples

Integrated Ocean Drilling Program (IODP) Expedition 346 drilled seven sites in August and September 2013 (Tada et al., 2015). Site

U1424 is located ~200 km southwest of Tsugaru Strait, near the boundary between the Japan and Yamato Basins ($40^{\circ}11.40'\text{N}$, $138^{\circ}13.90'\text{E}$, 2808 m below sea level, Fig. 1). Site U1425 is located in the central Sea of Japan at $39^{\circ}29.44'\text{N}$, $134^{\circ}26.55'\text{E}$, 1909 m below sea level. In this study, we selected and sampled tephras from the uppermost ~5 m of sediments of these two marine cores (Holes U1424A and U1425B) (Fig. 2; Table 1).

Two visible tephras at ~171–181 cm and ~ 283 cm were reported in Hole U1425B (Tada et al., 2015), and there is another tephra at 184–189 cm (Fig. 2). Stratigraphically, the uppermost tephra in Holes U1424A and U1425B is the ~30 ka AT (Aira-Tanzawa) tephra, which is a marker horizon for Sea of Japan sediments (Ikehara, 2015; Ikehara et al., 2004; Tada et al., 2015, 2018). There is a ~ 2 cm hiatus in between the tephras at 171–181 cm and 184–189 cm in Hole U1425B, and in the preliminary report (Tada et al., 2015), the tephra at 184–189 cm was not characterized, and the tephra at 283 cm was not correlated with known eruptions. The samples at ~480 to 489 cm are coarser-grained than the background sediments, and the number of glass shards was higher than the background number, suggesting that it is a cryptotephra (unpublished data). Therefore, three visible tephras, at 171–181 cm (samples at 174 cm, 177 cm, and 179 cm were selected for geochemical analysis), 184–189 cm (samples at 184 cm and 189 cm were selected for geochemical analysis), and 283 cm, together with a cryptotephra at 480–489 cm, were selected for geochemical analysis in this study.

In the preliminary report on the intervals sampled in this study, three visible tephras, including those tentatively correlated with AT (132–135.5 cm), Aso-4 (384–387 cm), Toya (463 cm), together with an uncorrelated tephra at ~241 cm, were identified in Hole U1424A (Fig. 2; Tada et al., 2018). Additionally, we observed three visible tephras in Hole U1424A, with various thicknesses less than 1 cm, at the depths of ~379 cm, ~381 cm, and ~ 398 cm, and all of these visible tephras were sampled for geochemical analysis.

In addition to these distal tephras, proximal tephra samples from the pre-Millennium eruption (NS-1, NS-2) of Changbaishan, as described in Sun et al. (2017), were sampled for geochemical analysis for comparison with the above distal tephras.

2.2. Electron micro-probe analysis (EPMA)

We analyzed the major element compositions of glass shards from distal tephras, using a JEOL JXA 8100 electron probe microanalyzer (EPMA, WDS), at the State Key Laboratory of Lithospheric Evolution of the Institute of Geology and Geophysics Chinese Academy of Sciences (IGGCAS) Beijing; and a JEOL JXA 8230 at the Wuhan Sample Solution Analytical Technology Company Limited, Wuhan, China. Ten elements (Na, Mg, Al, Si, K, Ca, Fe, Ti, Mn, P) were analyzed with an accelerating voltage of 15 kV, beam current of 10 nA, and beam diameter of 10 μm under a JEOL JXA 8100. Twelve elements (Na, Mg, Al, Si, K, Ca, Fe, Ti, Mn, P, Cl, S) were analyzed with an accelerating voltage of 15 kV, beam current of 6 nA, and beam diameter of 5 μm under a JEOL JXA 8230. The Na content was determined at the start of the analysis, and peak counting times were 20 s for all elements except for Na (10 s). We also analyzed MPI-DING fused secondary standard glasses, including ATHO-G and StHS6/80-G, to monitor data accuracy and precision (Jochum et al., 2006). All data are normalized to an anhydrous basis.

2.3. Laser ablation inductively coupled plasma mass spectrometry (LA-ICP-MS)

Trace element compositions of glasses from distal and proximal tephras were measured by LA-ICP-MS using an Agilent 7500 ICP-MS coupled to a COMPex Pro 193 nm Excimer laser-ablation system at IGGCAS. Data were obtained using a 24 μm spot size. Concentrations were calibrated using NIST SRM 612 with ^{29}Si as the internal standard which was determined by EPMA. During trace elements analysis, secondary standard glasses (ATHO-G, StHS6/80-G) were also analyzed to

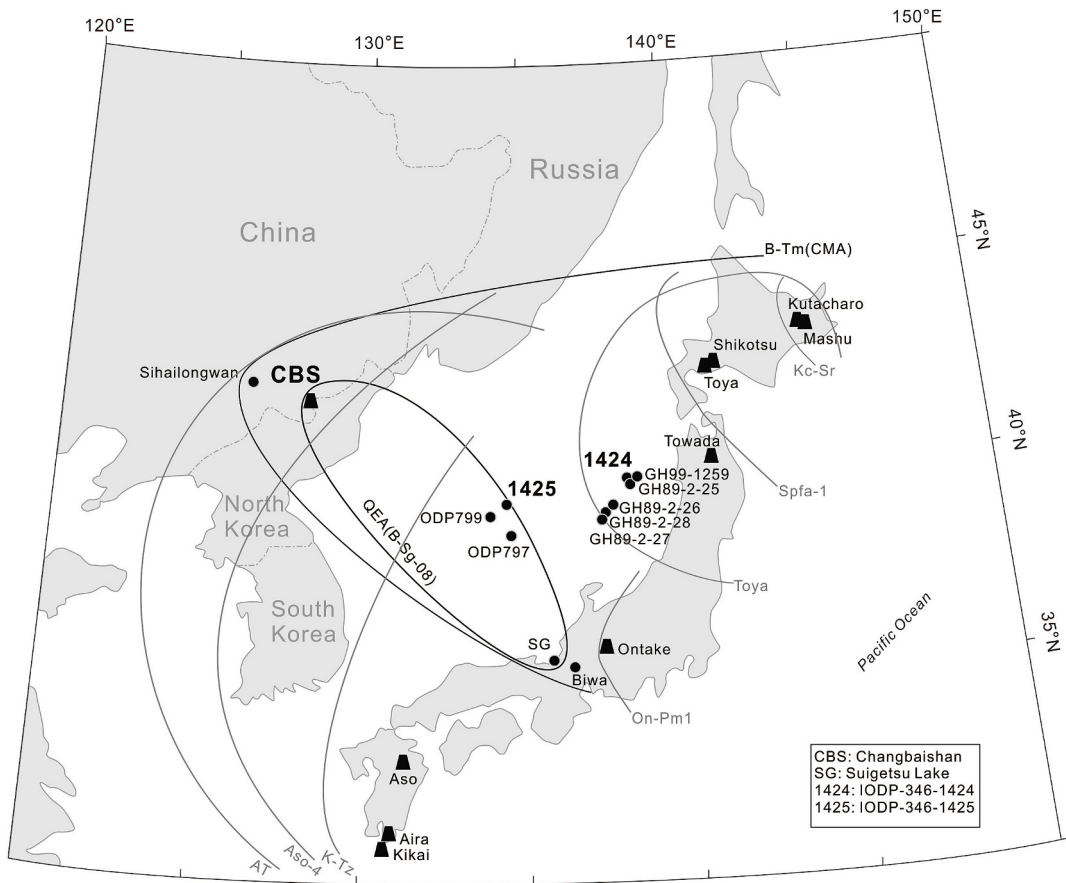


Fig. 1. Locations of Sites IODP-346-1424 and IODP-346-1425 analyzed in this study, and major volcanoes around northeast Asia. The major Late Pleistocene tephra dispersals and Changbaishan tephra dispersals are also shown.

monitor data accuracy and precision.

2.4. Age modelling

Age models for Holes U1424A and U1425B were constructed using Bayesian age-depth modelling based on the ages and stratigraphic positions of well-documented tephras, including AT, Aso-4, and Toya by Bacon software (Fig. 3 and Fig. 4) (Blaauw and Christen, 2011; Tada et al., 2018). We adopted the tephra ages of $30,009 \pm 189$ cal a BP for the AT tephra, constrained by radiocarbon dating of the sediments of Lake Suigetsu; 86.4 ± 1.1 ka for Aso-4, based on ^{40}Ar – ^{39}Ar dating; and 108 ± 19 ka for Toya, based on U–Th dating (Albert et al., 2019; Ito, 2014).

3. Results

Three visible tephra layers were recognized in IODP-346-1425B (i.e. IODP Cruise 346, Site 1425, and the same convention below). The first tephra is located at 184–189 cm and is named JS1425–189 according to start depth of tephra, and it was correlated with the AT tephra (Tada et al., 2018). The second tephra at ~283 cm is named JS1425–283, and the tephra at ~480–489 cm (JS1425–489) was not characterized by Tada et al. (2018).

Two visible tephra layers at ~132–135.5 cm (JS1424–135.5) and ~463 cm (JS1424–463) were correlated with the AT and Toya tephras, respectively (Tada et al., 2018). There is a small hiatus at ~380 cm within the confirmed Aso-4 tephra, noted by Tada et al. (2018), and we sampled the tephra at the depths of 379 cm (JS1424–379), 381 cm to 387 cm (JS1424–389). We also found an additional two tephra layers at ~241 cm (JS1424–241) and ~398 cm (JS1424–398) (Fig. 2 and Fig. 5).

3.1. Aira sourced tephras: JS1424–135.5, JS1425–181 and JS1425–189

The glass shards of JS1425–181 are homogeneous rhyolitic in composition ($n = 50$), with SiO_2 ranging from 77.53 wt% to 78.56 wt%, FeO from 0.91 wt% to 1.37 wt%, CaO from 0.99 wt% to 1.25 wt%, and K_2O from 3.02 wt% to 3.72 wt% (Fig. 6; Table 2; Table S1). The glass shard compositions of JS1425–189 exhibit a similar homogeneous chemistry ($n = 43$), with SiO_2 ranging from 77.46 wt% to 78.44 wt%, FeO from 1.11 wt% to 1.38 wt%, CaO from 1.03 wt% to 1.17 wt%, and K_2O from 3.08 wt% to 3.46 wt% (Fig. 6; Table 2; Table S1). The trace elements composition of JS1425–181 is relatively homogenous ($n = 7$, e.g., 9.10–12.70 ppm Th; 96.79–110.08 ppm Zr; 70.42–80.53 ppm Sr) (Figs. 6, 7; Table 3; Table S1). These geochemical compositions support the tentative correlation of tephra JS1425–181 to the AT tephra (Tada et al., 2018), and tephra JS1425–189 may also be from the same volcano considering its similar glass composition to the AT tephra. In the preliminary report the AT tephra was correlated to tephra JS1424–135.5 (Tada et al., 2018); hence, we did not conduct further geochemical analysis of this tephra, given that it is the most widespread confirmed marker horizon in the Sea of Japan during the study period.

3.2. Aso-4 tephra: JS1424–389, JS1425–489

Tephra JS1424–389 has a heterogeneous glass shards composition ($n = 34$), with 33 glass shards with SiO_2 ranging from 62.56 wt% to 73.22 wt%, FeO from 1.34 wt% to 6.06 wt%, CaO from 0.87 wt% to 4.27 wt%, and K_2O from 3.64 wt% to 5.14 wt% (Fig. 6; Table 2; Table S1). The trace elements composition of JS1424–379 is relatively homogenous ($n = 6$, e.g., 13.91–15.90 ppm Th; 257.92–356.38 ppm Zr;

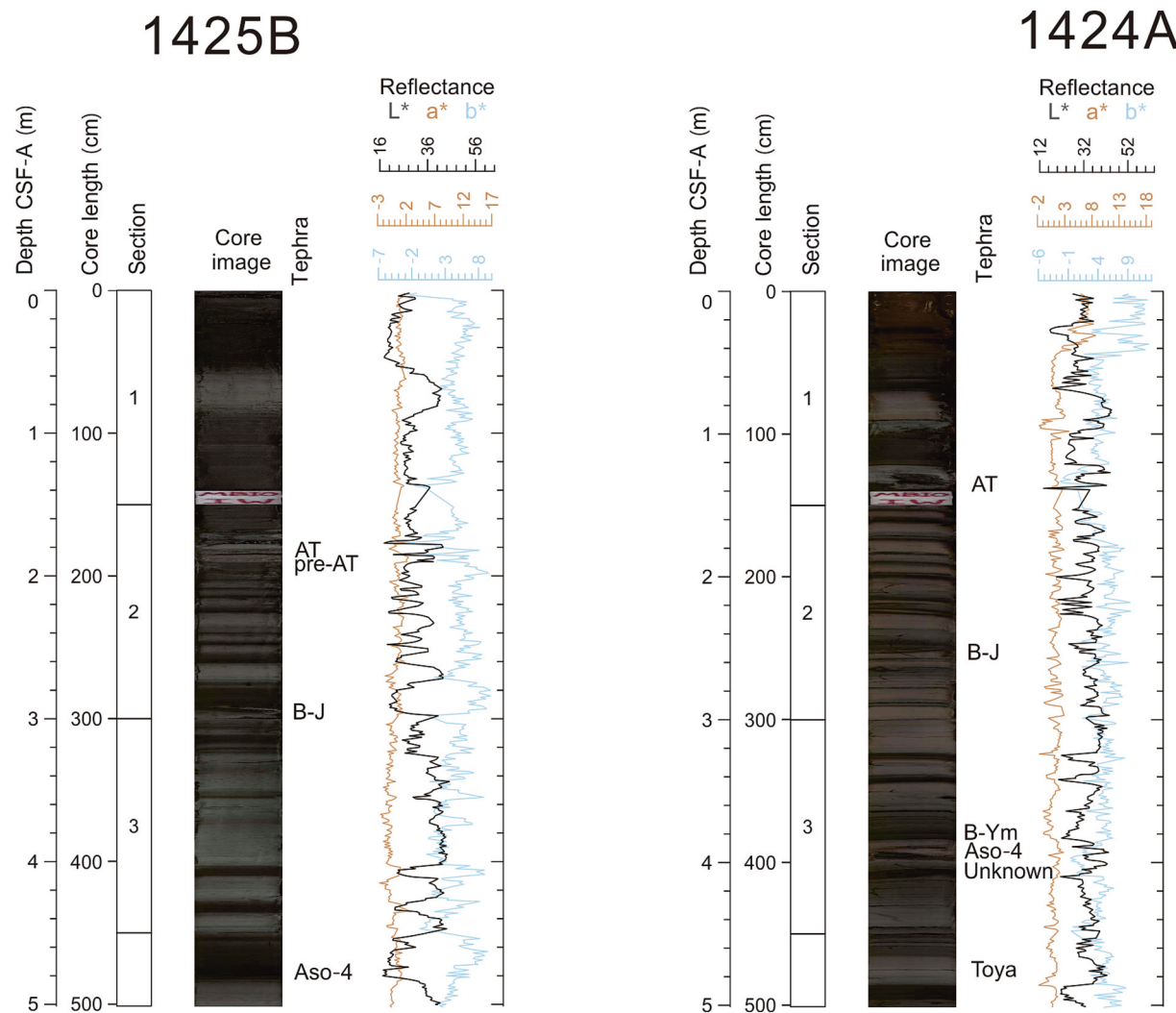


Fig. 2. Photos of sediment cores from IODP-346-1424 A and IODP-346-1425B. AT and Aso-4 are visible tephra that are widespread marker horizons in Sea of Japan sediments.

Table 1

Summary of the tephra recorded in the cores of IODP-346-U1424A and IODP-346-U1425B, the Sea of Japan.

Tephra Name	Depth (cm)	Glass composition (wt%)				Age (ka, 95 % level)	Correlation
		SiO ₂	FeO	K ₂ O	n		
JS1425-181	171–181	77.53–78.56	0.91–1.37	3.02–3.72	50	~30	Aira, AT
JS1425-189	184–189	77.46–78.44	1.11–1.38	3.08–3.46	43	30.7–29.8	Aira, A-Kn
JS1425-283	283	70.85–73.24	4.75–5.23	4.30–5.11	20	53.9–42.7	Changbaishan, Tianwenfeng
JS1425-489	480–489	60.22–73.50	1.42–8.55	2.50–4.53	103	~86	Aso, Aso-4
JS1424-135.5	132–135.5	–	–	–	0	~30	Aira, AT
JS1424-241	241	68.69–72.44	4.76–5.17	4.26–4.96	26	60.1–47.3	Changbaishan, Tianwenfeng
JS1424-379	379	67.35–71.11	4.17–5.17	4.57–5.31	42	87.3–81.8	Changbaishan, unknown
JS1424-389	381–389	62.56–73.29	1.34–6.06	3.64–5.14	69	~86	Aso, Aso-4
JS1424-398	398	71.43–74.08	1.36–2.04	4.36–5.16	16	92.0–86.1	Unknown
JS1424-463	463	77.78–78.58	0.85–1.04	2.67–4.34	15	~108	Toya

146.56–186.38 ppm Sr), while JS1424–384 and JS1424–387 have a heterogenous composition ($n = 10$, e.g., 8.78–18.89 ppm Th; 179.05–344.38 ppm Zr; 128.45–231.57 ppm Sr) (Figs. 6, 7; Table 3; Table S1). The mantle-normalized trace elements profile reveals that the glass shards are enriched in Rb relative to the HFSE, with depletions in Nb and Ta. Both major and trace elements compositions suggest that tephra JS1424–389 is from the same eruption, showing a close affinity to the glass shards of the Aso-4 tephra. What's more, there are 8 shards at the lower part of this tephra (387 cm) show trachytic glass

composition, different from the upper part with exclusive rhyolitic glass shards (381 cm and 384 cm; Table S1).

JS1425–489 also shows similar heterogeneous glass shard compositions to JS1424–389. Additionally, the trachytic glass shards are also present at the commencing lower part of the (e.g., 489 cm to 482 cm) tephra JS1425–489, while the no occurrence at the uppermost of this tephra (e.g., 481 cm to 480 cm). Such glass characteristics are consistent with the tephra of JS1424–389, confirming that the JS1425–489 is also from Aso-4 eruption.

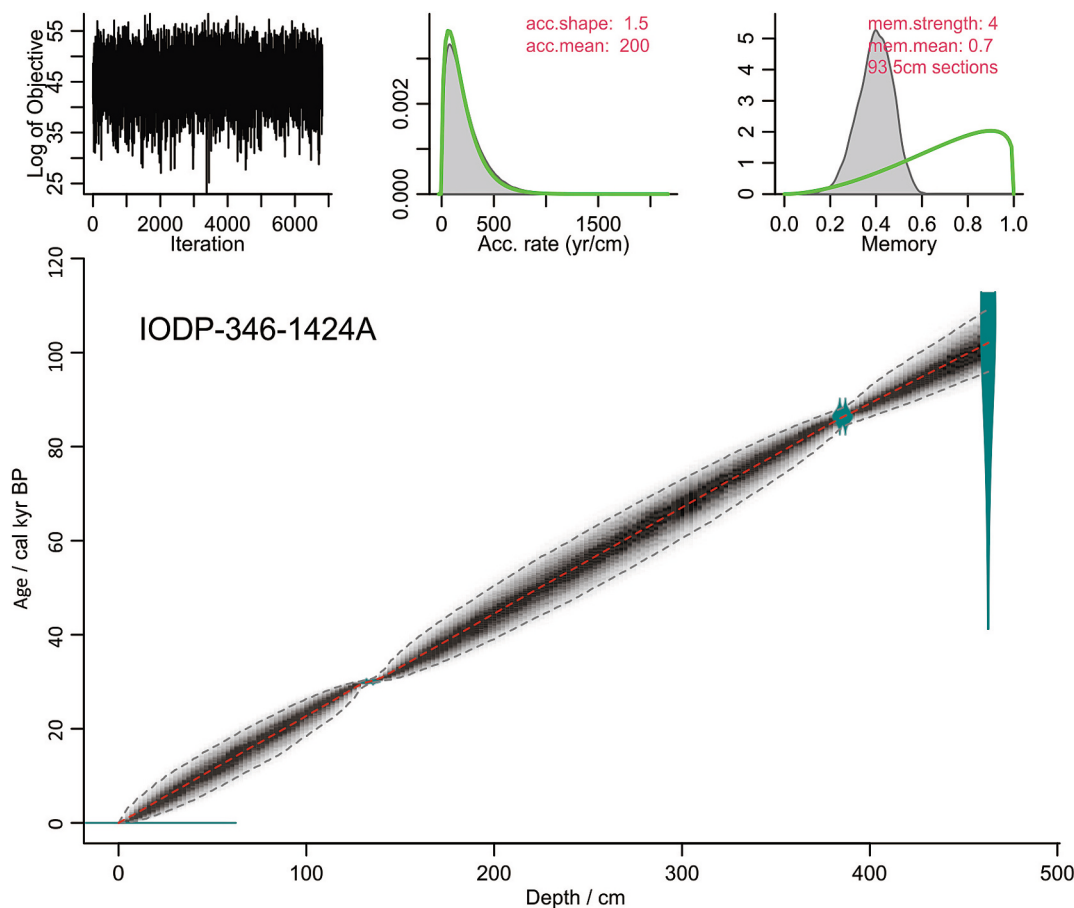


Fig. 3. Age model of the IODP-346-1424 A core, the Sea of Japan. The model was constructed using the ages of AT, Aso-4 and Toya.

3.3. JS1424–463: Toya tephra

The glass shards at 463 cm from IODP-346-1424 have a homogeneous rhyolitic composition in general, with 15 shards having SiO_2 ranging from 77.78 wt% to 78.58 wt%, FeO from 0.85 wt% to 1.04 wt%, CaO from 0.30 wt% to 0.40 wt%, and K₂O from 2.67 wt% to 4.34 wt% (Fig. 6; Table 2; Table S1). Additionally, there are two outlier shards with SiO_2 ranging from 73.66 wt% to 73.77 wt% (Table S1), which is very different from the known composition. The trace element compositions of the glass shards exhibit some degree of variability ($n = 4$, e.g., 4.81–7.32 ppm Th; 69.33–108.81 ppm Zr; 16.14–24.46 ppm Sr) (Figs. 6, 7; Table 3; Table S1). The glasses are enriched in Rb relative to the HFSE, with strong depletions in Nb and Ta. Such major and trace element compositions overlap with the Toya tephra very well.

3.4. JS1424–398: Unknown sourced tephra

The JS1424–398 tephra is characterized by the enrichment of microcysts and it has a relatively homogenous glass shard composition (Fig. 5; $n = 16$), with SiO_2 ranging from 71.43 wt% to 74.08 wt%, FeO from 1.36 wt% to 2.04 wt%, CaO from 1.38 wt% to 2.16 wt%, and K₂O from 4.36 wt% to 5.16 wt% (Fig. 6; Table 2; Table S1). The glass trace element compositions of this tephra were not determined because of the relatively small available surface areas for LA-ICP-MS analysis.

3.5. JS1424–241, JS1425–283: Changbaishan sourced tephra

The JS1424–241 tephra has a homogeneous rhyolitic glass shard composition ($n = 26$), with SiO_2 ranging from 68.69 wt% to 72.44 wt%, FeO from 4.76 wt% to 5.17 wt%, CaO from 0.27 wt% to 0.80 wt%, and

K₂O from 4.26 wt% to 4.96 wt% (Fig. 8; Table 2; Table S1). JS1425–283 has a similar homogeneous rhyolitic glass shard composition ($n = 20$), with SiO_2 ranging from 70.85 wt% to 73.24 wt%, FeO from 4.75 wt% to 5.23 wt%, CaO from 0.33 wt% to 0.54 wt%, and K₂O from 4.30 wt% to 5.11 wt% (Fig. 8; Table 2; Table S1). In contrast to the major element compositions, the glass trace element contents of JS1424–241 ($n = 7$, e.g., 52.91–72.23 ppm Th; 2746.64–3799.45 ppm Zr; 304.90–430.40 ppm Nb) and JS1425–283 ($n = 8$, e.g., 29.40–64.61 ppm Th; 1523.16–3485.81 ppm Zr; 182.20–393.02 ppm Nb) are heterogeneous (Figs. 7, 9; Table 3; Table S1). The glasses are characterized by the enrichment of LREE relative to HREE and pronounced depletions in Ba, Sr, and Eu, which is very different from the tephras from Japanese volcanoes in the sediment cores (e.g., the AT, Aso-4, and Toya tephras).

3.6. JS1424–379: Changbaishan sourced tephra

The glass shards from JS1424–379 have a consistent composition ($n = 42$), with SiO_2 ranging from 67.35 wt% to 71.11 wt%, FeO from 4.17 wt% to 5.17 wt%, CaO from 0.49 wt% to 1.07 wt%, and K₂O from 4.57 wt% to 5.31 wt% (Fig. 8; Table 2; Table S1). Like the major element compositions of the glass shards, the trace element contents of JS1424–381 are homogeneous ($n = 3$, e.g., 29.28–32.23 ppm Th; 1535.80–1845.73 ppm Zr; 245.11–277.72 ppm Rb) (Figs. 7, 9; Table 3; Table S1). The glasses in this tephra are also strongly depleted in Ba, Sr, and Eu, and enriched in LREE, relative to HREE.

3.7. Proximal Changbaishan Tianwenfeng tephra

The major element composition of NS-1 and NS-2 proximal tephras from Changbaishan volcano were characterized by Sun et al. (2017), and

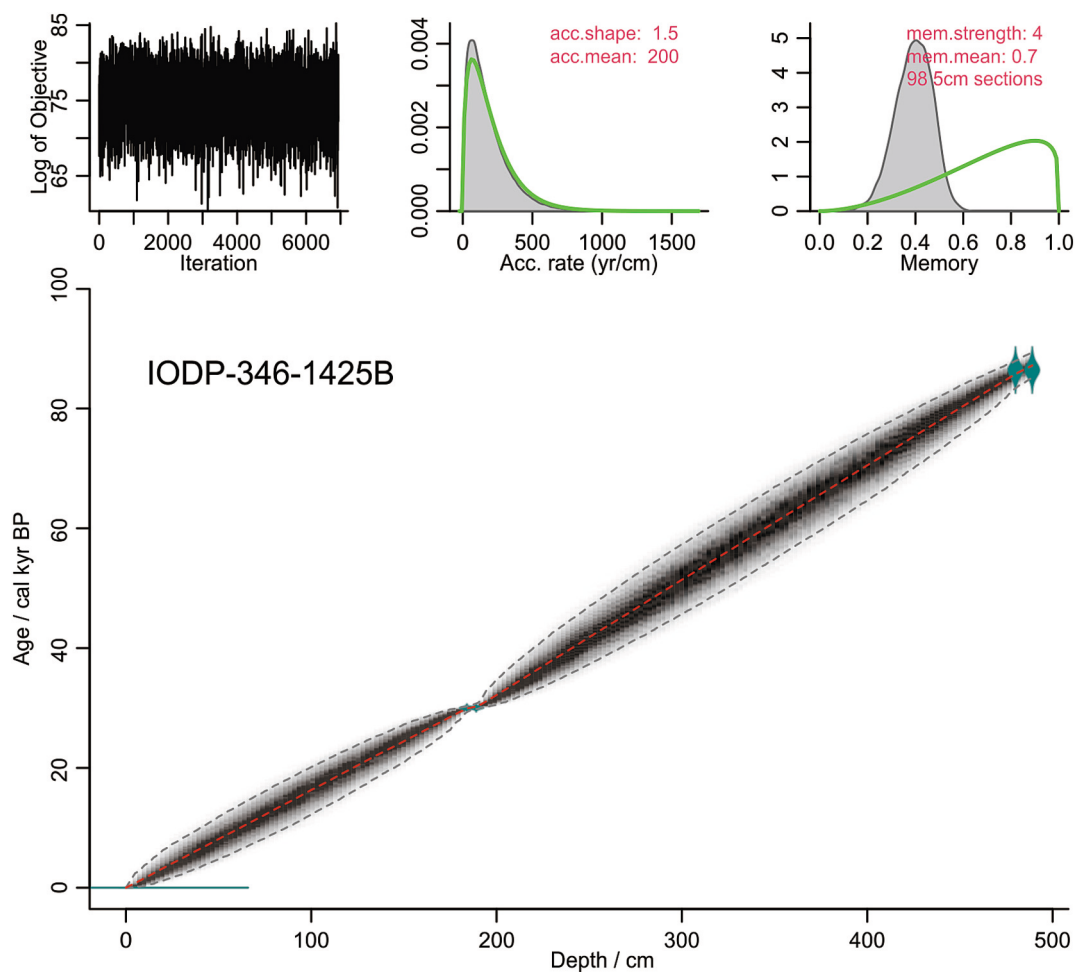


Fig. 4. Age model of the IODP-346-1425B core, the Sea of Japan. The model was constructed using the ages of AT and Aso-4.

we measured the trace element compositions of these two tephras in this study. NS-1 and NS-2 have similar heterogeneous major and trace element compositions (NS-1, $n = 12$ e.g., 27.47–85.56 ppm Th; 1619.74–1676.38 ppm Zr; 171.92–406.31 ppm Nb), and (NS-2, $n = 19$, e.g., 31.01–72.54 ppm Th; 1678.51–3807.83 ppm Zr; 199.62–421.89 ppm Nb) (Figs. 7, 9; Table 3; Table S1). They are characterized by pronounced depletions in Ba, Sr, and Eu, like the distal tephras.

3.8. Bayesian ages of the tephras in the sediment cores

Based on Bayesian age modelling, the JS1424–241 tephra recorded in Hole U1424A was dated to 60.1 to 47.3 ka (95 % probability), the JS1424–379 tephra to 87.3 to 81.8 ka (95 % probability), and JS1424–398 to 92.0 to 86.1 ka (95 % probability). The age of JS1425–283 recorded in Hole U1425B was constrained to 53.9 to 42.7 ka (95 % probability).

4. Discussion

4.1. Japan-sourced tephra marker layers

4.1.1. Aira caldera-sourced tephras

Aira caldera is located in southern Kyushu in Japan, and in ~29–28 cal ka BP it experienced one of the most violent explosive eruptions in its eruptive history, with VEI (Volcanic explosivity index) 7 (Machida and Arai, 2003; Machida, 1999). This eruption (Aira-Tanzawa) has been subjected to much age analysis, and radiocarbon dating of the organic material associated with this tephra yielded an age of 29,973–28,856 cal

a BP (95 % confidence interval, with the IntCal20 curve) (Miyairi and Yoshida, 2004; Reimer et al., 2020). High-resolution sedimentary archives have been used to refine the age of the tephra associated with this eruption: ages of 29,738 cal a BP and 29,682 cal a BP were obtained from Sihailongwan Maar Lake and Erlongwan Maar Lake, respectively, in northeast China (Mingram et al., 2008). Recently, the age of this eruption was refined to $30,009 \pm 189$ cal a BP (95 % confidence interval) based on the sedimentary chronology of Lake Suigetsu (Albert et al., 2019).

The Aira-Tanzawa eruption ejected $\sim 456 \text{ km}^3$ of material into the atmosphere, making it one of the largest eruptions in the eruptive history of Aira (Newhall et al., 2018). Tephra from this eruption, AT, has been widely used as a marker horizon from Japan Island to the Sea of Japan and even to Northeast and East China, and it is one of the most consistently-recorded tephra layers in Sea of Japan sediments (Eden et al., 1996; Machida and Arai, 2003; Machida, 1999; Mingram et al., 2008, 2018; Smith et al., 2013). This tephra, including proximal and distal records, has a highly homogeneous glass composition, and the tephra recorded in IODP-346-1425B (JS1425-171 to JS1425-181) also had similar glass compositions (Figs. 6, 7). Thus, these geochemical compositions provide reliable evidence for correlating this tephra to the AT eruption, and its age (e.g., $30,009 \pm 189$ cal a BP) can be transferred to these marine sediment cores.

It should be noted that the tephra of JS1425-184 to JS1425-189 also has similar glass compositions to JS1425-171 to JS1425-181, and there is a 2-cm hiatus in between these two tephras. Based on the sedimentation rate of the core, this represents a hiatus of several hundred years between them. Proximal exposures of the Aira caldera show that there

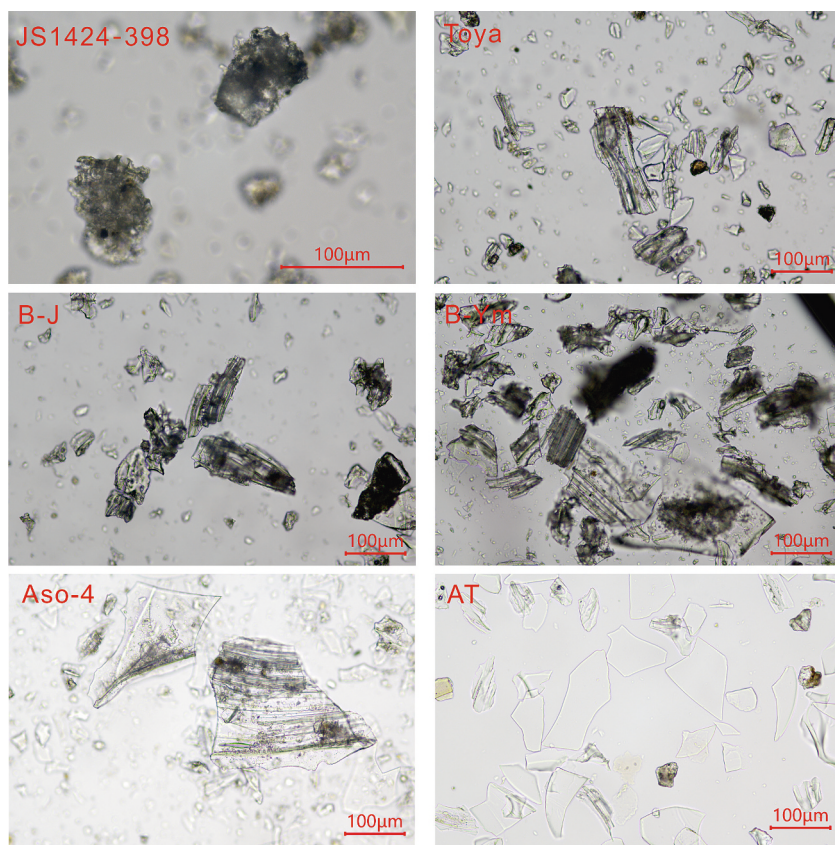


Fig. 5. Glass shard morphologies of the major tephrae recognized in this study.

were at least three eruptions in between the widespread ~30 ka AT tephra and the ~55 ka A-Iwato formation (A-Iw): represented by the Otsuka pumice fall deposit (A-Ot), the Fukaminato tephra Formation (A-Fm), and the Kenashino tephra Formation (A-Kn) (Machida and Arai, 2003). There are also numerous cryptotephrae recorded in the Lake Suigetsu pre-AT tephrae, such as SG14-2814, SG14-2856, and SG14-2873; and at Lake Biwa several AT-like visible tephrae are recorded before AT (McLean et al., 2020a, 2020b; Nagahashi et al., 2004; Satoguchi et al., 2008). Overall, these Aira-sourced tephrae show similar glass compositions. The age of the Kn tephra, ~29 ka, overlaps with the dating results of the AT tephra, while the A-Fm and A-Ot tephrae are dated to ~31 ka and 32.5 ka, respectively. The well-defined hiatus suggests that these two tephrae in core JS1425 are independent events, and it is likely that the tephra of JS1425-184 to JS1425-189 is correlative with the A-Kn tephra, considering the relatively brief hiatus between it and the AT tephra. The thickness of this pre-AT tephra in the Sea of Japan is ~5 cm, which implies that this tephra may have been transported much further than the central Sea of Japan. Therefore, the A-Kn tephra provides a new marker horizon to link the lacustrine sediments of central Japan Island to the marine sediments of the Sea of Japan, or even to more distal regions.

4.1.2. Aso caldera-sourced tephra: Aso-4

The Aso caldera is located in Kyushu, Japan, and it experienced several explosive eruptions with VEI 6–7, which contributed to the formation of the caldera, such as Aso-1 (250–270 ka), Aso-2 (~140 ka), Aso-3 (112.7 ka), and Aso-4 (Machida and Arai, 2003; Machida, 1999; Tsuji et al., 2018). The Aso-4 eruption is dated to ~70–90 ka based on various dating methods, and the orbitally-tuned marine oxygen isotope record has refined the age of this eruption to 86.8–87.3 ka; however, direct radiometric dating of the Aso-4 tephra has yielded more scattered results, e.g., fission track (FT, ~84 ka), K–Ar (89 ± 7 ka), TL (~71–78.4 ka), and ESR (~83 ka) dating (compiled by Aoki, 2008;

Machida, 1999). A tephra recorded in Lake Suigetsu (SG06–4963) was assigned the age of ~89 ka, similar to the K–Ar dating result; however, this age is relatively old because the tephra is located near the boundary of MIS 5a and MIS 5b (Machida and Arai, 2003; Smith et al., 2013). Recently, $^{40}\text{Ar}/^{39}\text{Ar}$ dating was conducted on proximal hornblende from the Aso-4 tephra, and an age of 86.4 ± 1.1 ka (2σ) was assigned to this eruption, which is consistent with the tuned marine oxygen isotopic age (Albert et al., 2019; Aoki, 2008). Consequently, we used this radiometric dating result as a marker point in the marine sediments of this study.

The Aso-4 eruption was the most violent explosive eruption during the eruptive history of the Aso caldera, and ~930–1860 km³ of bulk deposit (resulting in VEI 8) was erupted; It was one of the largest eruptions in the world over the past 100 ka (after the ~74 ka Toba eruption (Newhall et al., 2018; Takarada and Hoshizumi, 2020)). The tephra distribution axis of this eruption is likely to be in the northeast direction to the Aso caldera, and visible tephra from this eruption can be detected in northwest Pacific pelagic sediments ~2900 km away from the caldera, resulting in a tephra dispersal area of ~4,000,000 km² (Aoki, 2008; Machida and Arai, 2003; Machida, 1999). The Aso-4 tephra has a distinctive heterogeneous high potassium calc-alkaline glass shard composition which can be separated from other eruptions; several distal sites show that the Aso-4 tephra has a bimodal glass shard composition (e.g., Aoki, 2008; Ikehara, 2015; Smith et al., 2013). However, a recent proximal characterization revealed an additional component of the glass shards (Albert et al., 2019). The tephra in the marine sediment cores from the Sea of Japan of this study shows that the bimodal composition of the rhyolitic glass shards overlaps with previous published results, including proximal to distal Aso-4, which provides robust support for the correlation of these two tephrae with the Aso-4 eruption. However, these two Sea of Japan tephrae have no occurrence of the third component as defined by the proximal tephra, suggesting that the eruptive material corresponding to this component was not transported to the Sea of Japan.

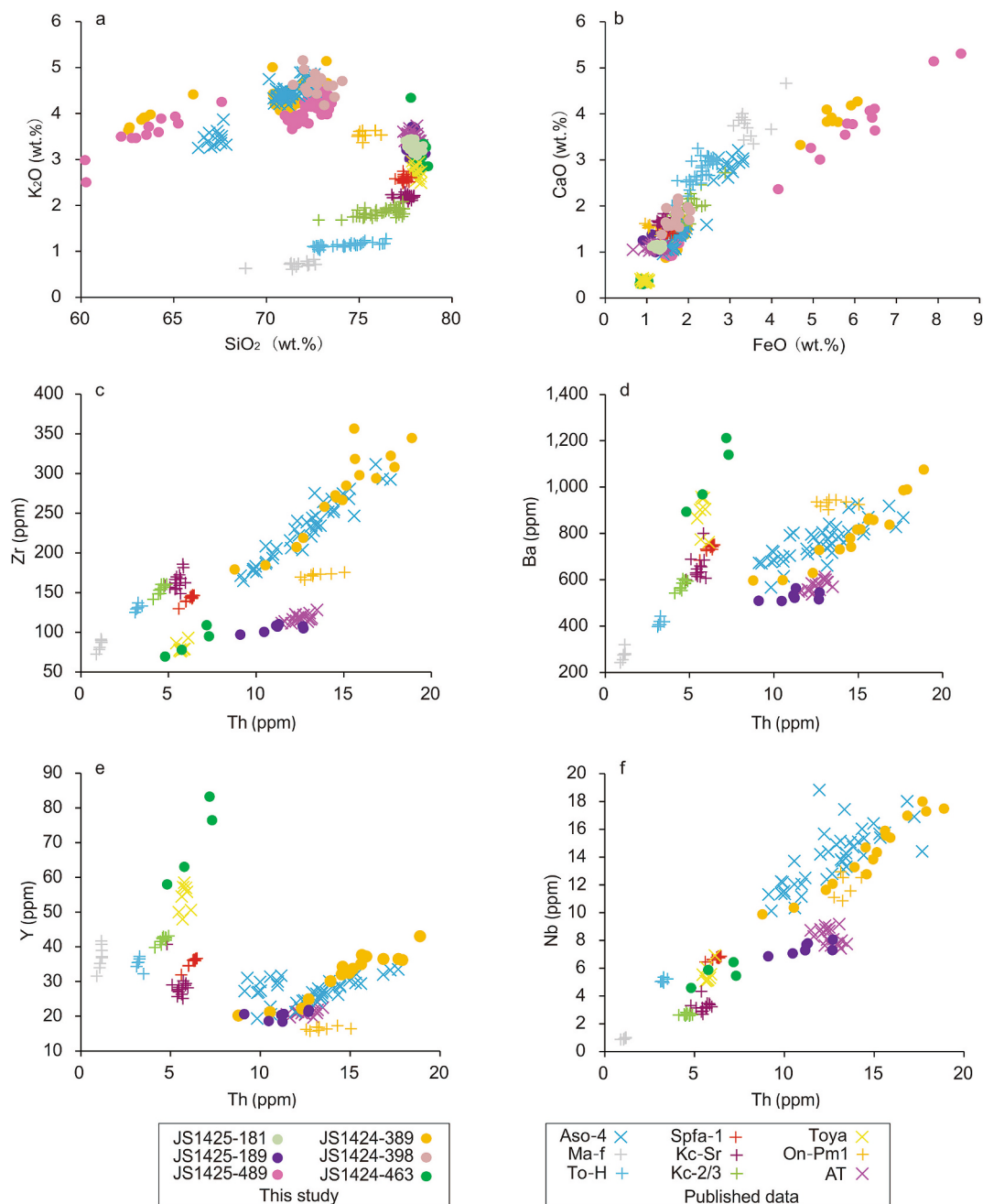


Fig. 6. Geochemical characterization including major and trace elements biplots of the glass shard compositions of the visible tephra of AT, Aso-4, and Toya recorded in IODP-346-1424 and IODP-346-1425, compared with the major Late Pleistocene tephra around Japan. Data sources: Albert et al. (2019); Smith et al., 2013.

Although the third component was not recognized in the Sea of Japan, our current results show that there is a previously unrecognized component with abundant less-evolved glass shards in the two sediment cores in this study (Fig. 6). The Aso-4 tephra is widespread across northeast Asia, but usually the distal tephra associated with this eruption has rhyolitic glass shard compositions and this tephra recorded in the Sea of Japan is also characterized by bimodal rhyolitic members which can be separated from other tephra (e.g., Aoki, 2008; Ikehara, 2015; Machida and Arai, 2003; Shirai et al., 1997; Smith et al., 2013). Our results provide the first evidence for a less-evolved glass member in distal records, which can be compared with the proximal Aso-4 tephra, suggesting that this member with less evolved glass shards is the primary member of the Aso-4 tephra (Keller et al., 2021).

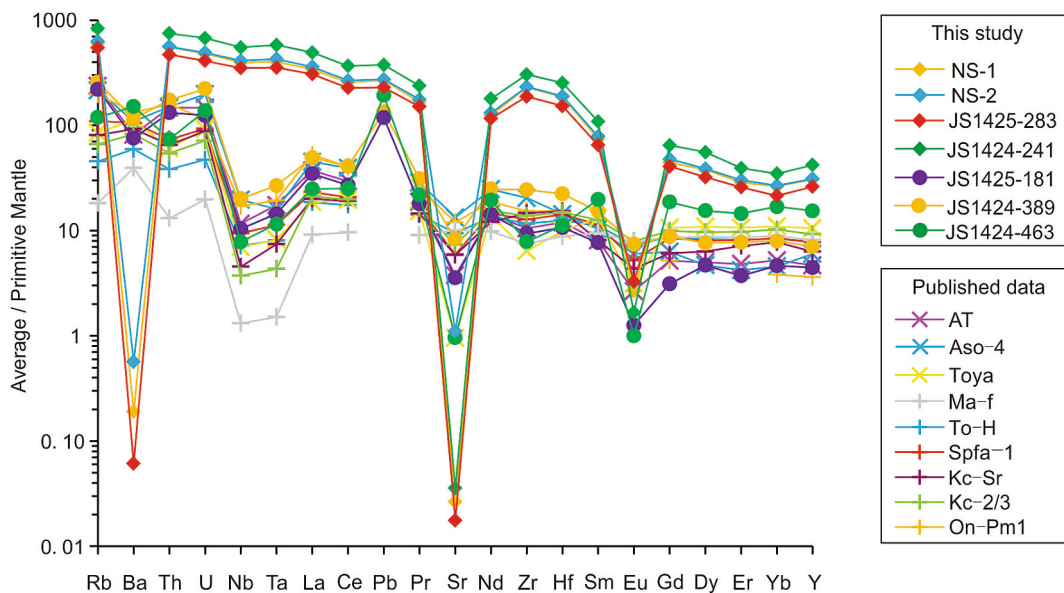
Previous studies have suggested that the Aso-4 eruption can be

divided into two subcycles fed by compositionally zoned mafic to silicic magma, and that there are also several materials that were generated by the mixing of mafic and silicic magma (Ishibashi et al., 2018; Kaneko et al., 2007; Keller et al., 2021). For the large explosive eruptions on a worldwide basis (e.g., Hildreth and Wilson, 2007; Liszewska et al., 2018), typically the evolved part of the magma was tapped before the less evolved magma, and thus the less-evolved eruptive materials should be deposited on top of the evolved material. In our marine sediment cores, these less evolved glass shards are enriched at the onset of the tephra in the Sea of Japan (e.g., at the depth at 387 cm at IODP-346-1424), and the number of these shards decreased to an almost undetectable level at the top of the tephra (e.g., at the depth at 381 cm at IODP-346-1424). This decreasing trend of less-evolved glass shards from the beginning to the end of the tephra also can be detected at Site

Table 2

Summary table of major and minor glass compositions of the tephras present by this study.

Tephra	JS1424–241		JS1424–379		JS1424–389		JS1424–398		JS1424–463		JS1425–181		JS1425–189		JS1425–283		JS1425–489	
	Mean	std																
SiO ₂	71.53	0.72	69.76	0.68	70.85	2.79	72.73	0.71	77.74	1.53	77.91	0.21	77.94	0.25	71.66	0.50	71.61	3.09
TiO ₂	0.30	0.06	0.34	0.05	0.48	0.16	0.16	0.06	0.05	0.04	0.14	0.03	0.14	0.03	0.32	0.04	0.47	0.17
Al ₂ O ₃	11.85	0.55	13.51	0.50	15.31	0.51	14.39	0.35	13.17	0.94	12.48	0.16	12.41	0.13	11.75	0.42	15.18	0.37
FeO _t	4.93	0.13	4.93	0.17	2.13	1.30	1.70	0.20	0.90	0.11	1.25	0.08	1.27	0.06	5.00	0.14	2.13	1.53
MnO	0.11	0.03	0.13	0.03	0.11	0.03	0.14	0.04	0.09	0.02	0.05	0.02	0.05	0.02	0.12	0.04	0.10	0.03
MgO	0.01	0.02	0.03	0.02	0.55	0.42	0.37	0.06	0.04	0.02	0.14	0.02	0.13	0.02	0.02	0.56	0.50	
CaO	0.44	0.11	0.65	0.10	1.55	0.90	1.77	0.22	0.40	0.16	1.12	0.06	1.11	0.03	0.42	0.06	1.40	0.94
Na ₂ O	5.85	0.24	5.67	0.38	4.50	0.41	3.72	0.16	4.60	0.84	3.59	0.15	3.65	0.10	5.76	0.27	4.33	0.31
K ₂ O	4.68	0.19	4.86	0.17	4.37	0.29	4.65	0.24	3.00	0.45	3.31	0.14	3.29	0.09	4.64	0.19	4.11	0.31
P ₂ O ₅	0.02	0.02	0.02	0.11	0.13	0.05	0.04	0.01	0.01	0.02	0.03	0.02	0.03	0.02	0.02	0.10	0.03	
Cl	0.31	0.05	0.24	0.03	0.12	0.02	0.37	0.05	—	—	—	—	—	—	0.31	0.04	—	—
SO ₃	0.04	0.03	0.03	0.03	0.07	0.04	0.02	0.03	—	—	—	—	—	—	0.04	0.03	—	—
n	26		42		69		16		15		50		43		20		103	

**Fig. 7.** Primitive mantle-normalized trace element compositions of glasses from Changbaishan proximal and distal tephras, together with the major Japan-sourced tephras (Albert et al., 2019).

IODP-346-1425. Therefore, the less evolved glass shards enriched at the onset of the distal tephra recorded in the two cores from the Sea of Japan cannot be fully explained by this zonation of the magma chamber of the Aso-4 eruption, considering that the early-stage materials are usually enriched in felsic glass shards and almost entirely lack less-evolved glass shards with SiO₂ content >67 wt% (e.g., Albert et al., 2019; Keller et al., 2021).

Less-evolved glass shards with SiO₂ content as low as ~62–63 wt%, comparable with our distal records from the Sea of Japan, were found in the late stage Aso-4 eruptive materials (19FK21m, Keller et al., 2021, 2023a, 2023b). Typically, the density of glass shards does not change significantly from medium to felsic glasses, and rhyolitic, trachytic, and even phonolitic glass shards can be extracted together by density separation with 2.5 g/cm³ sodium polytungstate (SPT) (e.g., Chen et al., 2019; Lane et al., 2015; McLean et al., 2018; Sun et al., 2015). This implies that the less-evolved glass shards in the distal tephra from the Sea of Japan are not completely controlled by density differences between evolved and less-evolved glasses. The size of the glass shards in these two cores can be up to 500 µm along the long axis, and they are almost colorless platy to pumiceous glasses (Fig. 5), which suggests that these parameters have limited impacts on the tephra loading. Therefore, glass density and morphology cannot result in sorting of those less evolved glass shards from late stage to be deposited at the commencing

part of distal tephra of Sea of Japan. Previous eruptions to Aso-4, such as Aso-3 has such less evolved glass shards, however, distal Aso-4 tephra records from Lake Suigetsu did not record such compositional glass shards (Albert et al., 2019; Aoki, 2008; McLean et al., 2020a, 2020b). If these less evolved glass shards were contaminated by previous eruptions, then they should be transported together with rhyolitic shards to distal regions. Therefore, we propose that the occurrence of these less-evolved glasses in the early stages of the Aso-4 eruption were primary melt part of this eruption, and these compositional shards might be transported to mainly further north to the Sea of Japan while limited to the northeast to the Lake Suigetsu and Pacific Ocean.

4.1.3. Toya-sourced tephra and an unknown-sourced tephra

The Toya caldera (~12 km × 12 km) is one of the volcanoes in the Shikotsu-Taya volcanic field situated in southwestern Hokkaido, Japan. This caldera was formed by a series of explosive eruptions at ~108 ka (Ito, 2014; Machida and Arai, 2003; Miyabuchi et al., 2014). During this eruption, ~150 km³ of bulk volcanic ash was transported and deposited around northern Japan, serving as a marker horizon around this region during the Late Pleistocene (Machida et al., 1987). This tephra is characterized by low FeO, low CaO, and moderate K₂O contents, and the exceptionally low CaO content distinguishes it from other tephras around Japan (Fig. 6). In the present study, the tephra at the depth of

Table 3
Summary table of trace glass compositions of the tephras including two proximal tephras from Changbaishan volcano and distal tephras from the Sea of Japan present by this study.

Tephra	NS-2		NS-1		JS1424-241		JS1424-379		JS1424-389		JS1425-283		JS1425-181			
	Mean	std	Mean	std	Mean	std	Mean	std	Mean	std	Mean	std	Mean	std		
Rb	419.95	93.58	380.44	133.81	526.46	53.74	260.48	16.38	163.14	25.94	75.47	7.99	346.95	89.66	139.77	2.87
Sr	1.09	0.57	0.67	0.37	0.88	0.59	4.71	5.76	174.49	25.32	20.28	3.48	0.59	0.13	75.33	3.73
Y	147.67	31.79	139.76	54.26	191.33	17.75	92.69	5.99	32.05	6.64	70.14	11.69	119.00	34.68	20.23	1.28
Zr	2732.32	605.50	2577.92	1017.63	3406.59	371.44	1676.34	156.97	273.76	53.63	87.62	17.64	2106.60	583.42	104.88	4.72
Nb	309.31	63.58	281.81	107.37	392.75	45.52	204.84	14.87	14.33	2.53	5.58	0.78	249.44	61.33	7.43	0.43
Ba	3.05	1.73	1.99	1.67	—	—	13.28	—	806.38	137.67	1052.87	147.43	3.41	—	527.49	20.51
La	260.35	54.26	234.62	74.11	337.70	35.22	162.32	13.92	33.94	5.80	17.08	3.68	211.29	56.84	23.82	1.60
Ce	497.90	103.54	453.63	146.35	650.22	71.38	313.70	21.44	72.64	13.69	44.42	5.63	402.05	102.59	48.01	1.93
Pr	51.08	10.31	45.73	14.51	65.65	6.95	32.50	2.75	8.56	1.61	6.02	1.16	41.64	11.52	4.96	0.87
Nd	186.77	40.22	168.25	53.99	242.71	23.33	122.89	5.35	33.62	5.42	26.37	3.39	157.58	40.68	19.21	3.57
Sm	36.70	8.21	32.96	11.09	48.28	5.44	24.69	4.88	6.77	2.36	8.79	2.23	28.82	7.22	3.98	0.83
Eu	0.57	0.25	0.60	0.23	0.65	0.25	0.45	0.31	1.33	0.48	0.67	—	0.73	0.18	0.37	0.27
Gd	29.91	6.63	26.36	10.14	38.50	3.91	17.43	1.07	5.99	2.61	11.13	2.87	24.35	9.15	6.49	1.27
Dy	29.99	6.94	28.00	10.87	41.03	3.88	20.35	2.41	5.61	1.99	11.39	2.42	23.75	6.83	4.03	0.85
Er	15.19	2.94	13.77	5.30	18.84	3.63	9.43	1.18	3.72	1.19	6.95	2.13	12.37	3.81	2.09	0.52
Yb	13.88	3.36	12.93	5.90	17.14	3.98	8.43	1.65	3.93	1.21	8.33	2.08	10.60	3.21	2.29	0.99
Hf	61.58	14.39	57.56	23.09	78.23	10.79	38.56	4.75	6.91	1.59	3.47	1.56	47.12	12.89	3.31	0.53
Ta	18.43	3.64	16.47	6.14	23.76	3.59	12.19	1.89	1.10	0.30	0.47	0.12	14.53	3.77	0.69	0.08
Pb	53.36	11.14	49.74	19.43	69.53	9.77	32.62	2.12	24.88	4.31	35.65	6.14	42.36	10.89	21.94	1.75
Th	50.08	11.46	47.30	18.68	63.59	6.58	29.09	3.24	14.74	2.68	6.27	1.20	39.86	10.55	11.23	1.25
U	10.82	2.45	10.06	3.97	14.16	1.87	6.05	0.91	4.67	0.96	2.89	0.63	8.62	2.64	2.61	0.39
n	19	—	12	7	—	3	—	16	4	—	8	—	7	—	—	—

463 cm at IODP-346-1424 (JS1424–463) has major and trace element compositions consistent with the proximal Toya tephra erupted at ~108 ka, which supports the tentative correlation by Tada et al. (2018), and indicates that the geochronological modelling using the age of this tephra is credible.

There are two glass shards with higher contents of CaO, Al₂O₃, and Na₂O in JS1424–463 than in the known Toya tephra (Table S1), which indicates that it was not sourced from the Toya eruption. These two shards cannot be correlated with known eruptions around this region, suggesting an unknown eruption with the same age as the Toya eruption. Future studies including cryptotephra records in this region and proximal records should be conducted to verify the source of this unknown eruption.

4.1.4. An 92.0–86.1 ka unknown eruption

The JS1424–398 tephra has similar FeO and CaO contents, implying that it is not from the intraplate Changbaishan volcano, and rather that it is from an arc volcano (Sun et al., 2018). Given its thickness, it is likely that this tephra is from Japan. An SiO₂ versus K₂O biplot is useful for differentiating tephras originating from northern and southern Japan, and on this biplot the JS1424–398 tephra exhibits a similar glass composition to the felsic member of the Aso-4 tephra, while the available Cl analyses from proximal and distal records show that the JS1424–398 tephra has a higher Cl content than the Aso-4 tephra (Fig. 10), indicating that that this tephra is not from the Aso caldera. The K₂O content of JS1424–398 glass is higher than 4.18 wt%, while those widespread Japanese tephras like AT and Toya exhibit less than 4.0 wt% K₂O content, excluding they were from the same eruption (Fig. 6; Table S1). IODP-346-1424 is close to highly active volcanoes, such as Towada, and Ontake; however, tephras from Towada typically have glass shards with a low K₂O content, which excludes it as the source volcano. One of the most widely distributed tephras from Ontake volcano is the On-Pm1, while its glass compositions are different from the JS1424–398 tephra (Fig. 6; Table S1), which implies that the Ontake-sourced tephras are not correlative with this tephra.

A visible tephra below the Aso-4 tephra and dated to ~99 ka is recorded at ODP Site 794, which is close to IODP-346-1424 (Shirai et al., 1997). The glass composition of the tephra recorded at ODP Site 794 (1H-3-104) has similar major element contents to JS1424–398 overall, while its MgO content is less than 0.2 wt% which is different from the JS1424–398 with MgO content higher than 0.25 wt% (Fig. 10). Shirai et al. (1997) did not cite secondary glass standard references to check their data precision, and we infer that these two tephras may have the same origin based on stratigraphic evidence from these two cores. There is a tephra layer named BT-30 at the depth of 33.00-m in the sediments of Lake Biwa, dated to ~99.5 ka (Nagahashi et al., 2004; Satoguchi et al., 2008). The rhyolitic member of this tephra shows a close glass compositional affinity to the JS1424–398 tephra and 1H-3-104 tephra recorded at ODP Site 794, except for the CaO content (Fig. 10). The composition of BT-30 was not validated with reference to secondary glass standards and was determined by the EDS (Energy Dispersive Spectrometers) method, which is different from the WDS (Wavelength Dispersive Spectrometers) method used in this study. The highly vesicular morphology of glass shards from JS1424–398 is also consistent with the BT-30 tephra in Lake Biwa (Nagahashi et al., 2004; Satoguchi et al., 2008), while it is very different from the platy or pumiceous shards from the AT- and Aso-4-sourced tephras (Fig. 5). Therefore, it is possible that JS1424–398 is correlative with the BT-30 tephra in Lake Biwa, suggesting that it is a new marker horizon for the area from the eastern Sea of Japan to central Japan Island. Future direct analysis by EPMA with precision checks with secondary glass standards on the Biwa tephra is needed to make a robust correlation.

4.2. Changbaishan-sourced tephras

JS1425–283, JS1424–241, and JS1424–379 have distinctive glass

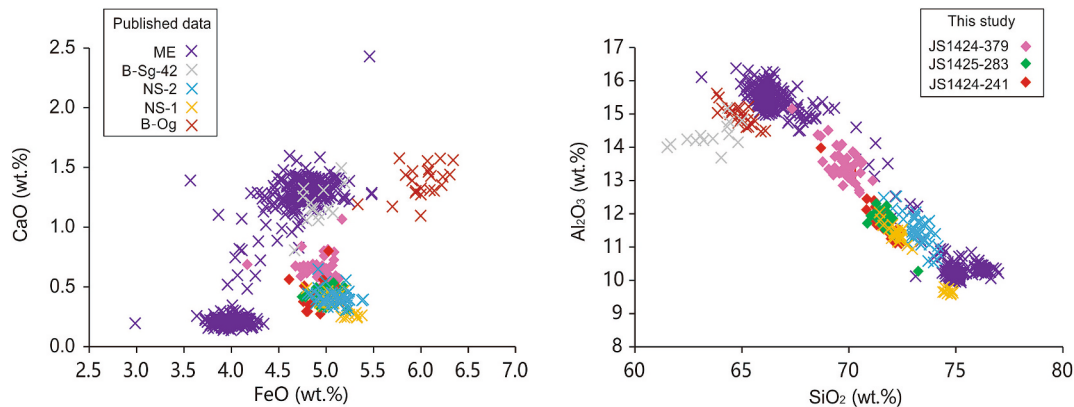


Fig. 8. Major element compositions of the glasses of the tephra from the Changbaishan Tianwenfeng eruption (Sun et al., 2017), and distal B-J and B-Ym tephra (this study), together with other major tephra from Changbaishan (Chen and Blockley, 2016; Derkachev et al., 2019; McLean et al., 2020; Sun et al., 2017).

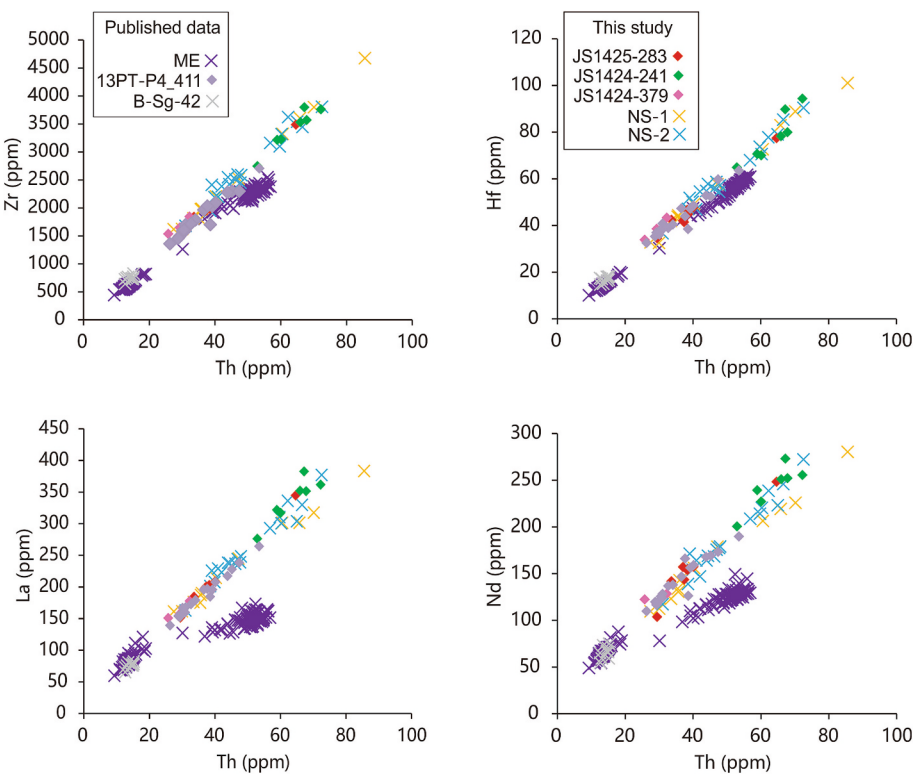


Fig. 9. Trace element compositions of glasses from tephra from the Changbaishan Tianwenfeng eruption, distal B-J and B-Ym tephra (this study), and other major tephra from Changbaishan (Chen and Blockley, 2016; McLean et al., 2020).

compositions, with high FeO and low CaO contents, which can be separated from those from Japan and the surrounding volcanic regions; however, they can be correlated with the Changbaishan-sourced tephras. Based on age models of the two cores in this study, the age of ~48.1 ka (53.9–42.7 ka, 95 % probability) was assigned to the JS1425–283 tephra; the age of ~53.7 ka (60.1–47.3 ka, 95 % probability) was assigned to the JS1424–241 tephra. These two tephra layers show a similar major elementary rhyolitic glass composition. During this period, there are two Changbaishan-sourced tephras: B-J (Baedusan–Japan Basin) with an age of 48–51 ka, recognized in Sea of Japan sediments; and B-Sg-42 dated to ~42 ka, identified in Lake Suigetsu (Ikehara et al., 2004; McLean et al., 2020a, 2020b). B-Sg-42 is a trachytic compositional tephra layer which is very different from JS1425–283 and JS1424–241 (Fig. 8); thus, the corresponding eruption cannot be from the same source as these two tephra layers. Therefore,

these two tephra layers can be correlated with the B-J tephra, considering the available major element compositions of the glass shards.

Additionally, we observed a difference between these two tephra layers recorded at IODP-346-1424 (JS1424–241) and IODP-346-1425 (JS1424–283): that is, JS1424–241 has more shards enriched in Zr, Th, Hf and other elements (i.e. it is a more evolved member), while JS1425–283 has only one shard with this enriched member and it consists predominantly of the less-evolved member with relatively low contents of Zr, Th, Hf, and other elements (Fig. 9; Table S1). It is likely that these two tephras have a heterogeneous trace elementary trend, which differs from the major elements generated homogeneous glass composition. The limited amount of trace analysis of the glass shards means that we cannot be sure if these two layers have fully overlapped trace element compositions, or if they are compositionally different. Therefore, there is the need for additional LA-ICP-MS analysis of glass

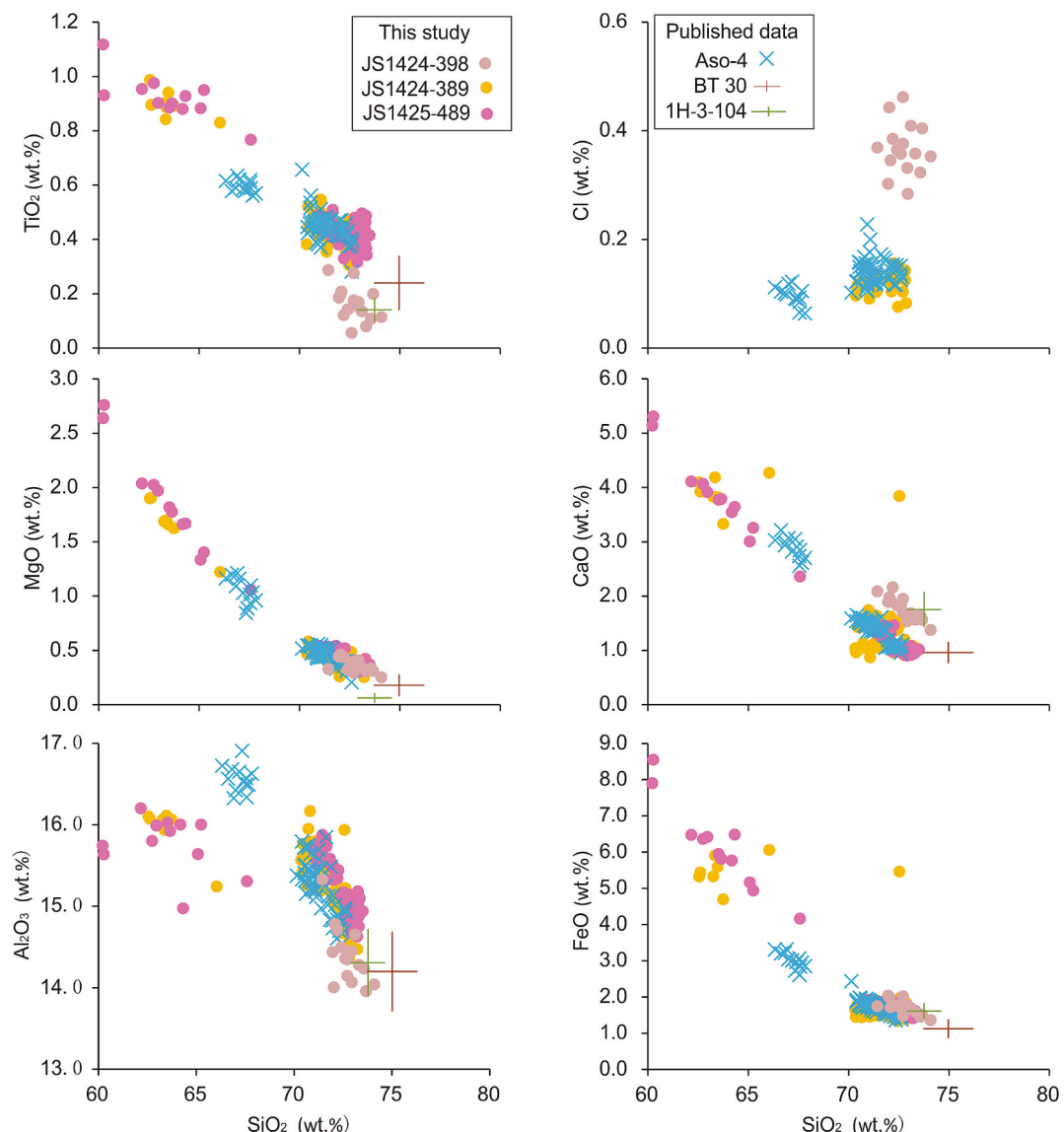


Fig. 10. Biplots comparing the Aso-4 tephra with the 1424–398, Bt30 recorded in Lake Biwa, and 1H-3-104 recorded in the Sea of Japan. Data sources: [Albert et al. \(2019\)](#); [Nagahashi et al. \(2004\)](#); [Shirai et al. \(1997\)](#).

shards from more sediment cores in the future to verify the geochemical complexity of this B-J tephra.

Stratigraphically, the JS1424-379 tephra is located just above the Aso-4 tephra (Fig. 2), as is also the case in tephrostratigraphic records from marine sediments from the Yamato Basin, Japan; examples, are cores GH89-2-28, GH89-2-26, and GH99-1259, where a cryptotephra layer of B-Ym (Baedusan-Yamato Basin) with an age of ~85.8 ka was detected just above the Aso-4 tephra (Fig. 3) ([Lim et al., 2013](#)). Additionally, JS1424-379 exhibits similar major element glass shard compositions to B-Ym reported from the Sea of Japan ([Ikehara, 2015](#); [Shirai et al., 1997](#)), confirming the correlation of JS1424-379 with B-Ym (Fig. 8). Geochemically, JS1424-379 has less evolved glass compositions than the B-J tephra, based on major elements; however, this tephra has a similar trace element composition to the less-evolved member of the B-J tephra.

4.3. Clarifying the Changbaishan explosive eruptions

4.3.1. Tianwenfeng eruption: 60.1–47.3/53.8–42.7 ka B-J tephra

At the proximal exposures around the northeast summit of Changbaishan caldera, there is a ~30-m thickness of pyroclastic fall deposits

(named the Tianwenfeng eruption) with gray to yellow fall pumice (NS-1 and NS-2, as defined by [Sun et al. \(2017\)](#)) covering the trachytic cone. The dating of this eruption is controversial. This thick tephra is covered by the Millennium eruption ash, indicating that it predates the Millennium eruption. [Yang et al. \(2014\)](#) assigned an age ~4 ka to this eruption, based on ⁴⁰Ar–³⁹Ar dating. Dating of the organic materials buried within the tephra was used to assign an age of ~4 ka to this eruption ([Liu et al., 1998](#)). However, the proximal lake sediment of Yuanchi Lake (~30 km to the east of Changbaishan caldera) has no tephra records between the Millennium eruption ash and the Qixiangzhan eruption ash, which challenges the suggestion that this was a Holocene eruption ([Sun et al., 2018](#)).

Tephrochronology has been used to constrain the timing of the Tianwenfeng eruption. [Wei and Gil \(2013\)](#) attempted to correlate this eruption with the unconfirmed ~24.5 ka B-V tephra recorded in the Sea of Japan, but this tephra is uncommon in Sea of Japan sediments, and [Wei and Gil \(2013\)](#) did not provide geochemical and geochronological evidence to support their correlation. [Derkachev and Utkin \(2019\)](#) reported the geochemical compositions of glass shards from the B-V tephra; however, its highly heterogeneous glass composition made it difficult to compare it with the NS-1 and NS-2 tephra, which

contradicts the correlation of the B-V tephra to the Changbaishan Tianwenfeng eruption. The distal B-J tephra was tentatively correlated with the Tianwenfeng eruption in previous studies; however, the distal and proximal data are not fully overlapped as there was no referenced standard glass for the published distal B-J glasses (Sun et al., 2017). Subsequent studies based on these published distal B-J tephras also tentatively correlated the Tianwenfeng eruption to the B-J tephra; however, the clear geochemical difference between them (e.g., differences in the contents of FeO, Na₂O, and TiO₂) does not support this correlation (See Fig. 7 in Pan et al., 2020).

In the present study, we compared both the proximal Tianwenfeng tephra (NS-1, NS-2) and the distal B-J tephra. These tephras exhibit different glass compositions, with a higher ratio of FeO to CaO from the major eruptions from Changbaishan; e.g., the Millennium eruption ash, B-Sg-42, and B-Og. The major and trace element contents of glass shards support the correlation of the distal B-J tephra with the Tianwenfeng tephra (NS-1, NS-2). Most of the Changbaishan tephras were transported to the east of the volcano; however, Millennium eruption ash has been found on the mainland of northeast China (Sun et al., 2015). The Sr–Nd isotopic composition of the sediments of Sihailongwan Lake, where the Millennium eruption ash was found, showed that there is a signal of an ash-fall event dated to ~47.3 ka, possibly correlative with Changbaishan volcanic products (Zaarur et al., 2020). The age of this event is very close to the age of the B-J tephra (60.1–47.3/53.8–42.7 ka) constrained in the present study, which implies that the ash from the Tianwenfeng eruption was transported to the interior of northeast China, forming a regional marker horizon to link high-resolution lacustrine sediments from northeast China to the marine sediments of the Sea of Japan.

It is interesting that distal cryptotephra records from the Sea of Japan show that Changbaishan experienced an explosive eruption at ~30 ka, which is significantly younger than the 60.1–47.3/53.8–42.7 ka B-J tephra. Shirai et al. (1997) detected a tephra with an age ~28 ka at ODP Site 794 in the Sea of Japan, and this tephra has a homogeneous glass shard composition consistent with the Tianwenfeng tephra (NS-1, NS-2). Subsequently, Chen et al. (2024) detected a cryptotephra (13PT-P4-411) in the southwestern Sea of Japan that could be correlated geochemically and geochronologically with this visible tephra at ODP Site 794. This ~30 ka tephra layer has a relatively heterogeneous glass major element composition compared to the homogeneous glass composition of the B-J tephra (Fig. 11). The glass geochemistry of the B-J tephra provides a better overlap with that of the Tianwenfeng tephra compared to 13PT-P4-411, suggesting that there was another major explosive eruption at ~30 ka that produced glass shards with a similar composition to the Tianwenfeng tephra.

4.3.2. 87.3–81.8 ka unknown eruption

Not only was JS1424–379 identified in IODP-346-1424 A, but the same sourced tephra was also found at ODP Site 794 and in cores

GH89–2–25, GH89–2–28, and GH99–1259 from the Sea of Japan (Fig. 1) (Shirai et al., 1997; Lim et al., 2013). This indicates that this tephra is a consistent marker horizon in this region. Until now, no known reported eruptions from Changbaishan were dated to ~90 ka, and thus this tephra layer should be from an unknown Changbaishan eruption. Future proximal tephra research should be conducted to verify its origin.

JS1424–379 represents a newly-discovered geochemically-characterized pyroclastic fall deposit from Changbaishan (Fig. 2 and Fig. 5). JS1424–379 with predominantly less-evolved glass shards can be clearly separated from the relatively evolved B-J tephra and Tianwenfeng tephra based on the major element compositions of the glass shards. However, the trace element compositions of glass shards cannot separate them clearly. At ODP Site 794, there is a visible tephra layer with an age of ~87 ka just above Aso-4, and its glass composition is consistent with that of JS1424–379 (Shirai et al., 1997). However, the B-Ym cryptotephra in cores GH89–2–25, GH89–2–28, and GH99–1259 has highly inconsistent glass compositions that are different from the relatively homogeneous JS1424–379 tephra, and even these three sediment cores show different glass compositions for the B-Ym tephra (e.g., the major elements of Al₂O₃, FeO, see Table 1 in Lim et al., 2013). The positions of the B-Ym tephra in cores GH89–2–25, GH89–2–28, and GH99–1259 are based on INAA core scanning analysis, the results of which may not be correlative with the occurrence of the highest number of glass shards, and thus the analysis of the tephras from these cores can be contaminated with other shards. We correlated the JS1424–379 to the B-Ym tephra when considering their consistent ages, and proposed that the B-Ym is consisted of homogeneous glass compositions because that the JS1424–379 recorded in IODP-346-1424 A and the 1H-3-79 recorded in ODP Site 794 share consistent homogeneous glass compositions and the tephras with highly heterogeneous glass compositions recorded in GH89–2–25, GH89–2–28, and GH99–1259 are highly possibly contaminated.

The B-Ym tephra is a stable visible marker layer in the eastern Sea of Japan, such the IODP-346-1424 A and ODP Site 794, while we cannot recognize the visible B-Ym in the IODP-346-1425B core. IODP-346-1424 A and ODP Site 794 are located to the east of Changbaishan volcano, but IODP-346-1425B is located to the southeast of Changbaishan volcano. Considering the occurrence of visible tephra, it appears that tephra from this eruption was mainly transported to the eastern direction of Changbaishan volcano, while southern dispersal of this eruption cannot be further than the site of IODP-346-1425B. Similarly, no visible tephra was identified at ODP Site 797, close to IODP-346-1425B (Shirai et al., 1997). Further studies of both proximal exposures and more distal tephras are needed to confirm if this is an extensive tephra layer, and cryptotephra analysis of IODP-346-1425B should be carried out to verify the dispersal limit of this tephra. Overall, the distribution of B-Ym is less extensive than that of the B-J tephra based on the occurrence of visible tephra in the Sea of Japan.

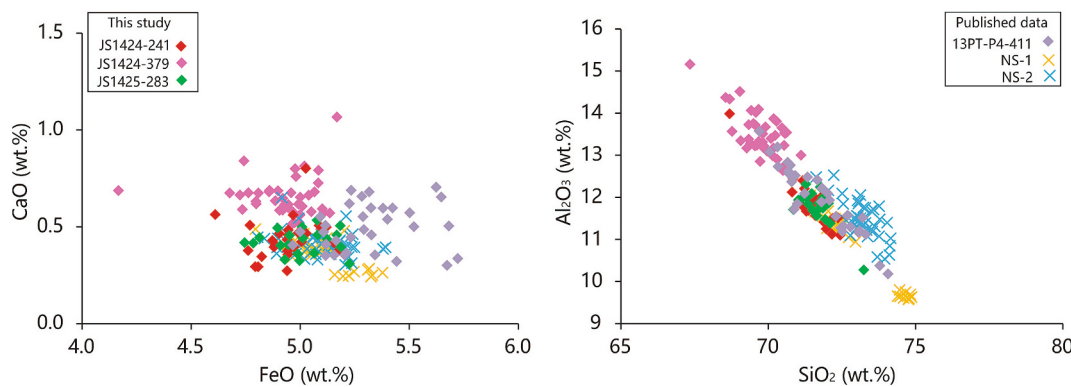


Fig. 11. Comparisons of the B-J tephra from the Changbaishan Tianwenfeng eruption (NS1, NS2; Sun et al., 2017) with the ~30 ka 13PT-P4-411 distal tephra from the Sea of Japan (Chen et al., 2024).

4.4. Implications for tephra correlations

Our findings demonstrate that the accurate determination of the minor element compositions of glass shards should be considered in tephra correlation. Based on the major element compositions of glass shards, JS1424–398 is difficult to separate from the Aso-4 tephra. However, the Aso-4 tephra usually exhibits a relatively low content of Cl (< 0.2 wt%), while the Cl content of JS1424–398 is >0.28 wt% (Fig. 10), thus excluding the Aso-4 eruption as the source for JS1424–398. Most of the tephras from highly active Japanese volcanoes have a low Cl content, such as Mashu, Kutacharo, Toya, Towada, Ontake, Aso, and Aira; while the Cl content of the glass from Daisen tephras is up to 0.4–0.5 wt % (Albert et al., 2018, 2019; Smith et al., 2013). However, the known Daisen-sourced tephras do not exhibit a consistent composition of other major elements compared to the JS1424–398 tephra, excluding the known Daisen eruption as the source of this distal tephra. It is likely that there were several unknown volcanic eruptions in Japan that generated high Cl-content glass shards. Overall, the Cl content of glass shards can be used to distinguish certain Japanese arc volcanoes.

5. Conclusions

Based on tephra records from the Sea of Japan we have identified seven major volcanic eruptions around northeast Asia over the past 100 ka, and the results provide insights into the eruptive processes of the volcanoes in this region. Japan-sourced tephras—AT (~30 ka), Aso-4 (~86 ka), and Toya (108 ka)—were confirmed geochemically. The pre-AT tephra, correlative with the A-Kn eruption of the Aira caldera, was identified in the Sea of Japan, and it is a new tephra layer that can be correlated to tephra records from Japanese lake sediments. For the Aso-4 tephra, we found a new component of glass shards but no occurrence of component 3 from the Sea of Japan, suggesting complex tephra dispersal and eruptive processes of the ~86 ka Aso-4 eruption. Additionally, a tephra layer with a rhyolitic glass composition dated to 92.0–86.1 ka was identified in the eastern Sea of Japan, which may be correlative with the BT-30 tephra recorded in Lake Biwa, providing a new marker horizon across the Sea of Japan to central Japan.

We confirmed and characterized two major explosive eruptions of Changbaishan volcano. First, we confirmed for the first time the correlation of the B-J tephra recorded in Sea of Japan with the Changbaishan Tianwenfeng eruption, based on the major and trace element composition of glass shards. An age of 60.1–47.3/53.8–42.7 ka was assigned to this eruption, based on age modelling of the marine sediment cores. Second, we geochemically characterized a new unknown eruption with an age of 87.3–81.8 ka using the B-Ym tephra recorded in the Sea of Japan. The B-J tephra is more widely distributed than the B-Ym tephra, based on the occurrence of these two tephra layers in the Sea of Japan, and the B-J tephra may be correlative with the volcanic event recorded in the sediments of Lake Sihailongwan in northeast China, suggesting that these tephra layers can serve as regional marker horizons.

CRediT authorship contribution statement

Jia Chen: Writing – original draft, Software, Methodology, Investigation. **Chunqing Sun:** Writing – review & editing, Writing – original draft, Supervision, Resources, Project administration, Methodology, Investigation, Funding acquisition, Data curation. **Yang Li:** Writing – review & editing, Visualization, Supervision. **Yuxin Chen:** Writing – review & editing, Validation, Software, Investigation. **Shuang Zhang:** Writing – review & editing. **Zhengfu Guo:** Writing – review & editing, Resources. **Jiaqi Liu:** Writing – review & editing, Resources.

Declaration of competing interest

The authors declare that they have no known competing financial interests or personal relationships that could have appeared to influence

the work reported in this paper.

Acknowledgements

This study was supported by the National Key Research and Development Project of China (2022YFF0802800), National Natural Science Foundation of China (41802253, 42072329), the Key Research Program of the Institute of Geology & Geophysics, CAS (IGGCAS-202204) and Strategy Priority Research Program (Category B) of Chinese Academy of Sciences (No. XDB0710000). Jan Bloemendal was thanked for English polishing. Sincerely thanks were extended to Kochi core center for providing marine sediments.

Appendix A. Supplementary data

Supplementary data to this article can be found online at <https://doi.org/10.1016/j.palaeo.2025.113219>.

Data availability

Data will be made available on request.

References

- Albert, P.G., Smith, V.C., et al., 2019. Geochemical characterisation of the late Quaternary widespread Japanese tephrostratigraphic markers and correlations to the Lake Suigetsu sedimentary archive (SG06 core). *Quat. Geochronol.* 52, 103–131.
- Albert, P.G., McLean, D., et al., 2024. Cryptotephra preserved in Lake Suigetsu (SG14 core) reveals the eruption timing and distribution of ash fall from Japanese volcanoes during the Late-glacial to early Holocene. *Quat. Sci. Rev.* 324, 108376.
- Aoki, K., 2008. Revised age and distribution of ca. 87ka Aso-4 tephra based on new evidence from the Northwest Pacific Ocean. *Quat. Int.* 178 (1), 100–118.
- Blaauw, M., Christen, J.A., 2011. Flexible paleoclimate age-depth models using an autoregressive gamma process. *Bayesian Anal.* 6 (3), 457–474.
- Bourne, A.J., Abbott, P.M., et al., 2016. Underestimated risks of recurrent long-range ash dispersal from northern Pacific Arc volcanoes. *Sci. Rep.* 6, 29837.
- Channell, J.E.T., Singer, B.S., et al., 2020. Timing of Quaternary geomagnetic reversals and excursions in volcanic and sedimentary archives. *Quat. Sci. Rev.* 228, 106114.
- Chen, X.-Y., Blockley, S.P.E., et al., 2016. Clarifying the distal to proximal tephrochronology of the Millennium (B-Tm) eruption, Changbaishan Volcano, northeast China. *Quat. Geochronol.* 33, 61–75.
- Chen, X.-Y., McLean, D., et al., 2019. Developing a Holocene tephrostratigraphy for northern Japan using the sedimentary record from Lake Kushu, Rebun Island. *Quat. Sci. Rev.* 215, 272–292.
- Chen, X.-Y., Xu, Y.-G., et al., 2024. Revisiting the Tianwen Yellow Pumice (TYP) Eruption of Changbaishan Volcano: Tephra Correlation, Eruption timing and its Climatostratigraphical Context. *J. Geophys. Res. Solid Earth* 129 (4) e2023JB028563.
- Davies, S.M., Albert, P.G., et al., 2024. Exploiting the Greenland volcanic ash repository to date caldera-forming eruptions and widespread isochrons during the Holocene. *Quat. Sci. Rev.* 334, 108707.
- Derkachev, A.N., Utkin, I.V., et al., 2019. Tephra layers of large explosive eruptions of Baitoushan/Changbaishan Volcano in the Japan Sea sediments. *Quat. Int.* 519, 200–214.
- Eden, D.N., Froggatt, P.C., et al., 1996. Volcanic glass found in late Quaternary Chinese loess: a pointer for future studies? *Quat. Int.* 34–36 (0), 107–111.
- Fattah, M., Stokes, S., 2003. Dating volcanic and related sediments by luminescence methods: a review. *Earth Sci. Rev.* 62 (3–4), 229–264.
- Hildreth, W., Wilson, C.J.N., 2007. Compositional zoning of the Bishop Tuff. *J. Petrol.* 48 (5), 951–999.
- Hughes, P.D.M., Mallon, G., et al., 2013. The impact of high tephra loading on late-Holocene carbon accumulation and vegetation succession in peatland communities. *Quat. Sci. Rev.* 67 (0), 160–175.
- Ikehara, K., 2015. Marine tephra in the Japan Sea sediments as a tool for paleoceanography and paleoclimatology. *Prog. Earth Planet. Sci.* 2 (1), 1–14.
- Ikehara, K., Kikkawa, K., et al., 2004. Origin and correlation of three tephras that erupted during oxygen isotope stage 3 found in cores from the Yamato Basin, central Japan Sea. *Q. Res. (Daiyonki-kenkyu)* 43 (3), 201–212.
- Ishibashi, H., Suwa, Y., et al., 2018. Amphibole–melt disequilibrium in silicic melt of the Aso-4 caldera-forming eruption at Aso Volcano, SW Japan. *Earth Planets Space* 70 (1), 137.
- Ito, H., 2014. Zircon U-Th-Pb dating using LA-ICP-MS: Simultaneous U-Pb and U-Th dating on the 0.1Ma Toya Tephra, Japan. *J. Volcanol. Geotherm. Res.* 289, 210–223.
- Jochum, K.P., Stoll, B., et al., 2006. MPI-DING reference glasses for in situ microanalysis: New reference values for element concentrations and isotope ratios. *Geochem. Geophys. Geosyst.* 7 (2), Q02008.
- Kaneko, K., Kamata, H., et al., 2007. Repeated large-scale eruptions from a single compositionally stratified magma chamber: an example from Aso volcano, Southwest Japan. *J. Volcanol. Geotherm. Res.* 167 (1–4), 160–180.

- Keller, F., Bachmann, O., et al., 2021. The Role of Crystal Accumulation and Cumulate Remobilization in the Formation of Large Zoned Ignimbrites: Insights From the Aso-4 Caldera-forming Eruption, Kyushu, Japan. *Front. Earth Sci.* 8.
- Keller, F., Guillong, M., et al., 2023a. Tracking caldera cycles in the Aso magmatic system – applications of magnetite composition as a proxy for differentiation. *J. Volcanol. Geotherm. Res.* 436, 107789.
- Keller, F., Popa, R.G., et al., 2023b. Variations in water saturation states and their impact on eruption size and frequency at the Aso supervolcano, Japan. *Earth Planet. Sci. Lett.* 622, 118400.
- Lane, C.S., Brauer, A., et al., 2015. The late Quaternary tephrostratigraphy of annually laminated sediments from Meerfelder Maar, Germany. *Quat. Sci. Rev.* 122 (0), 192–206.
- Lim, C., Toyoda, K., et al., 2013. Late Quaternary tephrostratigraphy of Baegdusan and Ulleung volcanoes using marine sediments in the Japan Sea/East Sea. *Quat. Res.* 80 (1), 76–87.
- Lindsay, J.M., Robertson, R.E.A., 2018. Integrating Volcanic Hazard Data in a Systematic Approach to develop Volcanic Hazard Maps in the Lesser Antilles. *Front. Earth Sci.* 6 (42).
- Liszewska, K.M., White, J.C., et al., 2018. Compositional and Thermodynamic Variability in a Stratified Magma Chamber: evidence from the Green Tuff Ignimbrite (Pantelleria, Italy). *J. Petrol.* 59 (12), 2245–2272.
- Liut, R.X., Wei, H.Q., et al., 1998. The Latest Eruptions from Tianshi Volcano, Changbaishan, Beijing.
- Liut, P., Yi, J., et al., 2023. Modelling the post-caldera plumbing system of Changbaishan volcano (China) from integrated geochemical, isotopic, geobarometric, and geophysical data. *Lithos* 454, 107287.
- Machida, H., 1999. The stratigraphy, chronology and distribution of distal marker-tephras in and around Japan. *Glob. Planet. Chang.* 21 (1–3), 71–94.
- Machida, H., Arai, F., 2003. *Atlas of Tephra in and Around Japan*. University of Tokyo Press, Tokyo.
- Machida, H., Arai, F., et al., 1987. Toya ash-a widespread late quaternary time-marker in Northern Japan. *Q. Res. (Daiyonki-Kenkyu)* 26 (2), 129–145.
- Mackay, H., Hughes, P.D.M., et al., 2016. A mid to late Holocene cryptotephra framework from eastern North America. *Quat. Sci. Rev.* 132, 101–113.
- McLean, D., Albert, P.G., et al., 2016. Identification of the Changbaishan ‘Millennium’ (B-Tm) eruption deposit in the Lake Suigetsu (SG06) sedimentary archive, Japan: Synchronisation of hemispheric-wide palaeoclimate archives. *Quat. Sci. Rev.* 150, 301–307.
- McLean, D., Albert, P.G., et al., 2018. Integrating the Holocene tephrostratigraphy for East Asia using a high-resolution cryptotephra study from Lake Suigetsu (SG14 core), Central Japan. *Quat. Sci. Rev.* 183, 36–58.
- McLean, D., Albert, P.G., et al., 2020a. Refining the eruptive history of Ulleungdo and Changbaishan volcanoes (East Asia) over the last 86 kyr using distal sedimentary records. *J. Volcanol. Geotherm. Res.* 389 (1), 106669.
- McLean, D., Albert, P.G., et al., 2020b. Constraints on the timing of explosive volcanism at Aso and Aira calderas (Japan) between 50 and 30 ka: New insights from the Lake Suigetsu sedimentary record (SG14 core). *Geochemistry 21* (8) (Geophysics, Geosystems n/a(n/a): e2019GC008874).
- Mingram, J., Frank, U., et al., 2008. A widespread East Asian chronomarker (Aira-TN tephra) found in varved maar lake sediments (Sihailongwan and Erlongwan). In: Of the LongGang Volcanic Field (NE China). 3IMC Conference. Malargüe, Argentina.
- Mingram, J., Stebich, M., et al., 2018. Millennial-scale East Asian monsoon variability of the last glacial deduced from annually laminated sediments from Lake Sihailongwan, N.E. China. *Quat. Sci. Rev.* 201, 57–76.
- Miyabuchi, Y., Okuno, M., et al., 2014. Tephrostratigraphy and eruptive history of post-caldera stage of Toya Volcano, Hokkaido, northern Japan. *J. Volcanol. Geotherm. Res.* 281 (0), 34–52.
- Miyairi, Y., Yoshida, K., et al., 2004. Improved 14C dating of a tephra layer (AT tephra, Japan) using AMS on selected organic fractions. *Nuclear Inst. and Methods in Phys. Sec. B: Beam Interactions with Mater. and Atoms* 223–224, 555–559.
- Nagahashi, Y., Yoshikawa, S., et al., 2004. Stratigraphy and Chronology of Widespread Tephra Layers during the past 430ky in the Kinki District and the Yatsugatake Mountains: Major Element Composition of the Glass Shards using EDS Analysis. *Q. Res. (Daiyonki-Kenkyu)* 43 (1), 15–35.
- Newhall, C., Self, S., et al., 2018. Anticipating future Volcanic Explosivity Index (VEI) 7 eruptions and their chilling impacts. *Geosphere* 14 (2), 572–603.
- Pan, B., de Silva, S.L., et al., 2020. Late Pleistocene to present day eruptive history of the Changbaishan-Tianshi Volcano, China/DPRK: New field, geochronological and chemical constraints. *J. Volcanol. Geotherm. Res.* 106870.
- Rawson, H., Naranjo, J.A., et al., 2015. The frequency and magnitude of post-glacial explosive eruptions at Volcán Mocho-Choshuenco, southern Chile. *J. Volcanol. Geotherm. Res.* 299, 103–129.
- Reimer, P.J., Austin, W.E.N., et al., 2020. The IntCal20 Northern Hemisphere Radiocarbon Age Calibration Curve (0–55 Cal Kbp). *Radiocarbon* 1–33.
- Satoguchi, Y., Nagahashi, Y., et al., 2008. The Middle Pleistocene to Holocene tephrostratigraphy of the Takashima-oki core from Lake Biwa, Central Japan. *J. Geosci. Osaka City Univ.* 51 (6), 47–58.
- Shirai, M., Tada, R., et al., 1997. Identification and Chronostratigraphy of Middle to Upper Quaternary Marker Tephras Occurring in the Anden Coast based on Comparison with ODP Cores in the Sea of Japan. *Q. Res.* 36 (3), 183–196.
- Singer, B.S., Jicha, B.R., et al., 2014. Geomagnetic field excursion recorded 17ka at Tianshi Volcano, China: New 40Ar/39Ar age and significance. *Geophys. Res. Lett.* 41 (8), 2794–2802.
- Smith, V.C., Staff, R.A., et al., 2013. Identification and correlation of visible tephras in the Lake Suigetsu SG06 sedimentary archive, Japan: chronostratigraphic markers for synchronising of east Asian/west Pacific palaeoclimatic records across the last 150 ka. *Quat. Sci. Rev.* 67 (0), 121–137.
- Sun, C., Plunkett, G., et al., 2014. Ash from Changbaishan Millennium eruption recorded in Greenland ice: Implications for determining the eruption’s timing and impact. *Geophys. Res. Lett.* 41 (2), 694–701.
- Sun, C., You, H., et al., 2015. New evidence for the presence of Changbaishan Millennium eruption ash in the Longgang volcanic field, Northeast China. *Gondwana Res.* 28 (1), 52–60.
- Sun, C., Liu, J., et al., 2017. Tephrostratigraphy of Changbaishan volcano, Northeast China, since the mid-Holocene. *Quat. Sci. Rev.* 177, 104–119.
- Sun, C., Wang, L., et al., 2018. Ash from the Changbaishan Qixiangzhan eruption: a new early Holocene marker horizon across East Asia. *J. Geophys. Res. Solid Earth* 123 (8), 6442–6450.
- Sun, C., Wang, L., et al., 2021. An integrated Late Pleistocene to Holocene tephrostratigraphic framework for South-east and East Asia. *Geophys. Res. Lett.* 48 (5) e2020GL090582.
- Sun, C., Plunkett, G., et al., 2022. Four widespread East Asian tephra marker horizons during early MIS 3: ~60–50 ka tephrostratigraphy of Huguangyan Maar Lake southern China. *Quat. Sci. Rev.* 279, 107389.
- Sun, C., Plunkett, G., et al., 2024. Major Holocene cryptotephra layers identified from Jeju Island, Republic of Korea: Implications for regional volcanic eruptions and environmental changes. *Palaeogeogr. Palaeoclimatol. Palaeoecol.* 655, 112530.
- Tada, R., Murray, R., et al., 2015. Proceedings of Integrated Ocean Drilling Program. IODP.
- Tada, R., Irino, T., et al., 2018. High-resolution and high-precision correlation of dark and light layers in the Quaternary hemipelagic sediments of the Japan Sea recovered during IODP Expedition 346. *Prog. Earth Planet. Sci.* 5 (1), 19.
- Takarada, S., Hoshizumi, H., 2020. Distribution and Eruptive Volume of Aso-4 Pyroclastic Density Current and Tephra Fall Deposits, Japan: A M8 Super-Eruption. *Front. Earth Sci.* 8.
- Tsuji, T., Ikeda, M., et al., 2018. High resolution record of Quaternary explosive volcanism recorded in fluvio-lacustrine sediments of the Uwa basin, southwest Japan. *Quat. Int.* 471, 278–297.
- Vineberg, S.O., Albert, P.G., et al., 2024. A detailed record of large explosive eruptions from Japan between ~120 and 50 ka preserved at Lake Suigetsu. *Quat. Sci. Rev.* 346, 109021.
- Wei, H., Gil, J., 2013. Eruptive History of Tianshi Volcano, Changbaishan, Northeast China: Process and Hazard. *Forecasting Volcanic Activity - Reading and Translating the Messages of Nature for Society*. Kagoshima, Japan, p. 802.
- Wei, H., Liu, G., et al., 2013. Review of eruptive activity at Tianshi volcano, Changbaishan, northeast China: implications for possible future eruptions. *Bull. Volcanol.* 75 (4), 1–14.
- Yang, L., Wang, F., et al., 2014. 40Ar/39Ar geochronology of Holocene volcanic activity at Changbaishan Tianshi volcano, Northeast China. *Quat. Geochronol.* 21, 106–114.
- Zaarur, S., Stein, M., et al., 2020. Synoptic stability and anomalies in NE China inferred from dust provenance of Sihailongwan maar sediments during the past ~80 kyr. *Quat. Sci. Rev.* 239, 106279.
- Zhang, M., Guo, Z., et al., 2015. Late Cenozoic intraplate volcanism in Changbai volcanic field, on the border of China and North Korea: insights into deep subduction of the Pacific slab and intraplate volcanism. *J. Geol. Soc. Lond.* 172 (5), 648–663.
- Zhang, M., Guo, Z., et al., 2018. The intraplate Changbaishan volcanic field (China/North Korea) and its active Tianshi (Paektu, Baekdu) caldera: a review on eruptive history, magma origin and evolution, geodynamic significance, recent dynamics and potential hazards. *Earth Sci. Rev.* 187, 19–52.